Karlsruher Institut für Technologie
Institut für Technische Physik

INVESTIGATION OF POWER GRID TECHNOLOGIES FOR OFFSHORE WIND FARM SYSTEMS

Masterarbeit
im Studiengang Elektrotechnik

durchgeführt und vorgelegt von:

Mauro Nafarrate B. Sc.

Aufgabensteller: Dr. Mathias Noe

Zweitgutachter: Dr. Yingzhen Liu

Tutor: Fabian Schreiner

Bearbeitungszeit: Zeitraum

Karlsruhe, 24. Januar 2019

Karlsruhe Institute of Technology

Institute for Technical Physics
Supra Group

08 Februar 2019

Master Thesis

Investigation of collection grid topologies for offshore windfarm systems

Description

To reduce the Levelized Cost of Energy a continuous growth in size and power of offshore wind farms can be observed during the last years. Superconducting technology can meet the requirements of higher power ratings while enabling a compact, lightweight and easy design.

To provide long distance and high power transmission to the onshore grid, several high voltage direct current links (HVDC) are already installed or planed in projects. Moreover, there are some feasibility studies about an offshore DC collection grid between each wind turbine. However, all the wind turbines are connected with AC technology and the approach of a DC collection grid has not been tested yet.

The purpose of this work is a technical comparison of the existing AC connection systems and potential DC collection topologies regarding the principal feasibility and the overall system efficiency.

The work shall include the following work packages:

- Extensive literature research and comparison of existing and potential grid topologies
- Modeling of selected grid topologies with appropriate software (e.g. MATLAB Simulink , DIgSILENT Power Factory)
- Development of evaluation criteria like efficiency, weight, stability or power quality to compare the different models

Qualification

Candidates should have some basic knowledge in power grids and the modeling of power grids.

Starting date and duration

Immediately after agreement, short term, 6 months

Contact person

Fabian Schreiner
✉ fabian.schreiner@kit.edu
Institute for Technical Physics

Yingzhen Liu
✉ yingzhen.liu@kit.edu
Institute for Technical Physics

Index

Declaration of academic honesty

Hereby I declare that the present thesis is drawn up by myself without help of third parties but the support of my supervisor, that all used sources and tools including the internet are completely and exactly mentioned, and that everything is marked which is taken unchanged, shortened or analogous from other literature.

Karlsruhe, January 24, 2019.

Abstract

In the present document, an investigation about offshore wind farm technology is presented. The main objective of the work is to investigate the possibility of the farm to work in Direct Current instead of the conventional Alternate Current. With this in mind model of an AC wind farm is simulated in Simulink, in order to compare its performance with a DC wind farm model.

In order to create those, the current technology of wind turbines is first presented. The different elements that form a turbine are explained and the generator used in the models selected and analytically designed.

Next, the different types of wind farms are listed. The AC and DC technologies are explained and the wind farm topologies presented. A simple configuration is selected for the simulation.

On the next chapter, the electronic converters, one of the most important element of the system are presented. The current technologies and the models for the DC wind farm are explained and the topologies for the simulation designed.

Finally, the simulated models are described. These are then simulated and the results obtained are used to compare them. A final conclusion is made afterwards.

List of figures

List of Tables

Symbols and Abbreviations

Latin symbols

	Meaning	Unit
E_w	Energy of the wind	J
m	Mass	kg
v_w	Speed of the wind	m/s^2
A	Area	m^2
t	Time	s
P_w	Power carried by the wind	W
c_p	Power coefficient of the turbine	-
R	Radius of the turbine blades	M
m	Masse	kg
P_m	Mechanical power of the turbine	W
n_{turb}	Rotational speed of the turbine	rpm
N_p	Number of pole pairs of the generator	-
q	Number of slot per pole per phase	-
B_{rm}	Remanent magnetic flux of the magnets	T
m	Number of phases	-
r_s	Stator radius	M
D_s	Diameter of the air gap	m
h_{sy}	Height of the stator yoke	mm
h_{ry}	Height of the rotor yoke	mm
l_m	Magnet height	mm
k_{sfill}	Slot filling factor	-
l_{ext}	Length of the exterior armature	m

Greek Symbols

	Meaning	Unit
ρ	Density of air	kg/m^3
ω_{turb}	Rotational speed of the turbine	Rad/s
λ_{opt}	Optimal tip speed ratio	-
μ_0	Magnetic permeability of vacuum	H/m
μ_{rm}	Active recoil permeability of the magnets	-
ρ_{Cu}	Resistivity of copper	µΩm
τ_p	Pole pitch	mm

Abbreviations

	Meaning	Unit
AC	Alternate Current	-
DC	Direct Current	-
SCIG	Squirrel Cage Induction Generator	-
WECS	Wind Energy Conversion System	-
DFIG	Doubly Fed Induction Generator	-
WRSG	Wound Rotor Synchronous Generator	-
PMSG	Permanent Magnet Synchronous Generator	-
VSC	Voltage Source Converter	-
IGBT	Insulated Gate Bipolar Transistor	-
LCOE	Levelized Cost of Energy	€/kWh
HTS	High Temperature Superconductors	-
HVDC	High Voltage Direct Current	-
HVAC	High Voltage Alternate Current	-
DD	Direct Drive	-
STATCOM	Static Synchronous Compensator	-
PCC	Point of Common Coupling	-
MVAC	Medium Voltage Alternate Current	-
WT	Wind Turbine	-
MOSFET	Metal Oxide Semiconductor Field Effect Transistor	-
PWM	Pulse Width Modulation	-
RMS	Root Mean Square	-

1 Introduction

The relevance of wind power as a power source is increasing worldwide. In 2016, a capacity of 55 GW was installed all over the world. Moreover, the trend suggests that the development of the industry is going to continue for the next years [1] . In order to achieve it, the wind industry is searching for improved ways of generating electricity.

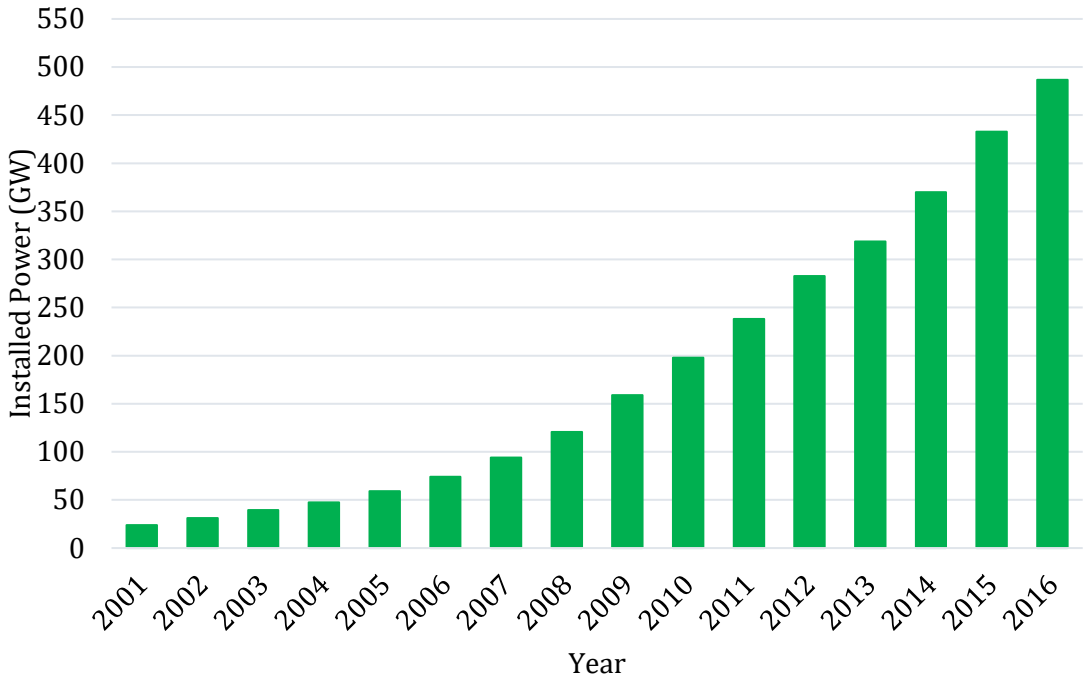

FIG. 1 Cumulated capacity of installed wind turbines [4]

Through the development of the wind industry, the size of the wind turbines has been increasing steadily. The development of the wind turbine power rating over the last 15 years is shown in in FIG. 2 and a forecast for 2030 is made.

This way the Levelized Cost of Energy (LCOE) is lowered. This value measures the lifetime costs divided by the produced energy. Thus, a bigger turbine would have higher installation costs, but with more power, it would create more energy.

If 10 years ago the mean power of installed turbines was 2MW, that number has increased to 5MW. The actual portfolio of many manufacturers already presents much bigger turbines. The evolution of the size of the turbines is also depicted in FIG. 2 Evolution of offshore wind turbine power rating and forecast [8]

Another recent variation includes offshore locations, where the turbines are installed far from the coast. Some advantages are found there, like higher mean wind speed and less interferences from terrain.

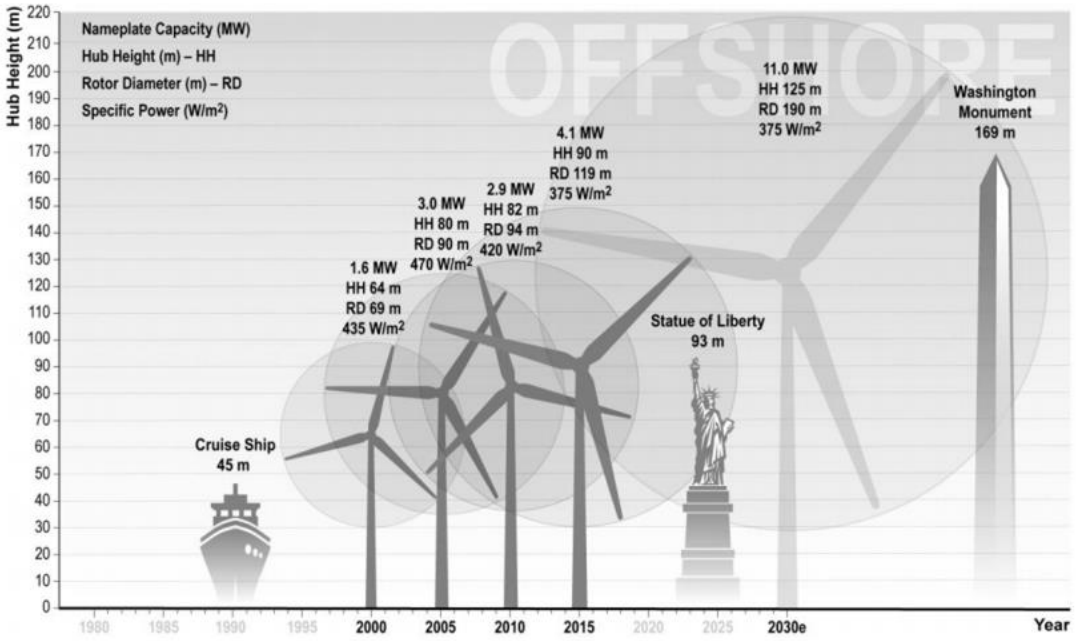

FIG. 2 Evolution of offshore wind turbine power rating and forecast [8]

In addition, the offshore location means bigger turbines are easier assembled than onshore. Actual boat technology is able to transport and install heavy components in a simpler way than it is done onshore. The usually mountainous locations add difficulty in onshore locations.

Nevertheless, offshore wind farms present many challenges. The location means a harsh environment and a long distance for the energy to the final electricity consumer. There is no possibility for overhead lines on sea and AC undersea cables can create big capacitive reactive power needs.

Due to the distance to the shore, connection from offshore wind farms is sometimes made in High Voltage Direct Current, or HVDC, subsea cables that present no such problems. The current technology is based in a large number of turbines connected to an offshore substation. This substation then transports the electricity to the shore by means of DC One or more turbine clusters can be connected to the same substation [7] [9]

Moreover, the whole collection grid of the wind farm could be made in DC, to decrease losses and make it easier to transport the energy to the shore. The challenges that this idea presents are discussed on the present work.

To sum up, for offshore wind farms, the installation costs are much higher than onshore, but the produced energy is higher, making it more and more attractive. In addition to the bigger turbines and the offshore farms, other ideas are being investigated. Such as the elimination of the gearbox or more efficient technologies.

According to one of these ideas, High Temperature Superconductors (HTS) can be used in the generators. The use of superconductors presents an opportunity to decrease the size of the conducting material in the generator. Thus, the machine is smaller and lighter. For high power turbines like these ones, the saving in weight is significant. Hence, the use of superconducting materials is being studied, but the challenges are great.

The machine that is being designed in our institute creates DC voltage and current, unlike the established technology in which both generator and grid work in AC. For this reason, the current technology that has been used for a long time is no longer applicable and the DC grids need to be studied from scratch.

Indeed, there was no need for high power DC converters to be studied and designed, since DC grids are usually used in two ways, for low power applications such as, house appliances or information electronics, or as previously stated HVDC transmission lines, where this kind of technology is not needed, as is explained in section 4.

2 Wind Turbine Technology

In this chapter, an introduction to the Wind Energy Conversion Systems, or WECS, is made. As well as an overview of the most common generator topologies and systems.

2.1 Wind energy conversion systems

The working principle of a wind turbine is relatively simple. The machine transforms the kinetic energy of the moving air into rotational mechanical energy, the energy on the shaft. This rotational energy is then transformed through the generator into electric energy.

According to [2] in ancient times, the wind energy was used, although not for creating electricity. The windmills were used for grinding seeds, as water pumps or as different purpose machines. With the beginning of industrialization, they were substituted with combustion engines or electrical machines powered from the grid.

Only in the 70´s, with the petrol price crisis, the interest of using wind to create electricity greatly increased. The first prototypes were created at the beginning of the 20th century, but from this moment on, the technology would be used in a major industry.

The most common design has its origin in Denmark, where it was developed in the 50's. It has become the standard of the industry. The design consists on a horizontal axis wind turbine with three blades and an orientable nacelle. There are many other different designs, but they are much less common.

2.1.1 Physics of the WECS

The operation of the turbine is based in the lift principle, in which the blade design makes the wind create a force perpendicular to the drag, the lift, which makes the blades turn. A scheme of this principle is shown in FIG. 3.

The wind carries an energy E_v that is proportional to its speed v_w, the area of the rotor A, the density of the incoming air ρ and the time t, in which the calculation is made. Thus the energy is

$$E_v = \frac{1}{2}mv^2 = \frac{1}{2}(Avt\rho)v^2 = \frac{1}{2}\rho Atv^3 \qquad (2.1.1.)$$

On the other hand, power is energy per unit of time, so the power incident on the surface of the rotor P_w is:

$$P_w = \frac{1}{2}\rho A v^3 \qquad (2.1.2.)$$

This is the total power that goes into the wind turbine, however, it is not possible to extract it all. There are losses as turbulence or drag. Hence, a power coefficient c_p is included.

This calculation takes into account that the wind speed out of the turbine cannot be zero, so there is a limit on the power that can be extracted from the wind. This theoretical limit was discovered by Betz, in 1926 [10] . This limit is applied as:

$$P_{Betz} = \frac{1}{2}\rho A v^3 c_{pBetz} = \frac{1}{2}\rho A v^3 0.59 \qquad (2.1.3.)$$

Therefore, the maximum power that can be extracted is only a 59% of the incoming winds power. In truth, this value is always lower, due to turbulence and mechanical losses. Modern turbines can achieve 50% [2] .

Nevertheless, the basic working principle of the blades is the lift principle. The idea is that the blade shape is made in a way that an angle with the incoming wind is created. This angle makes the wind move quicker in the upper part than in the lower part, thus creating a pressure difference that makes the rotor turn.

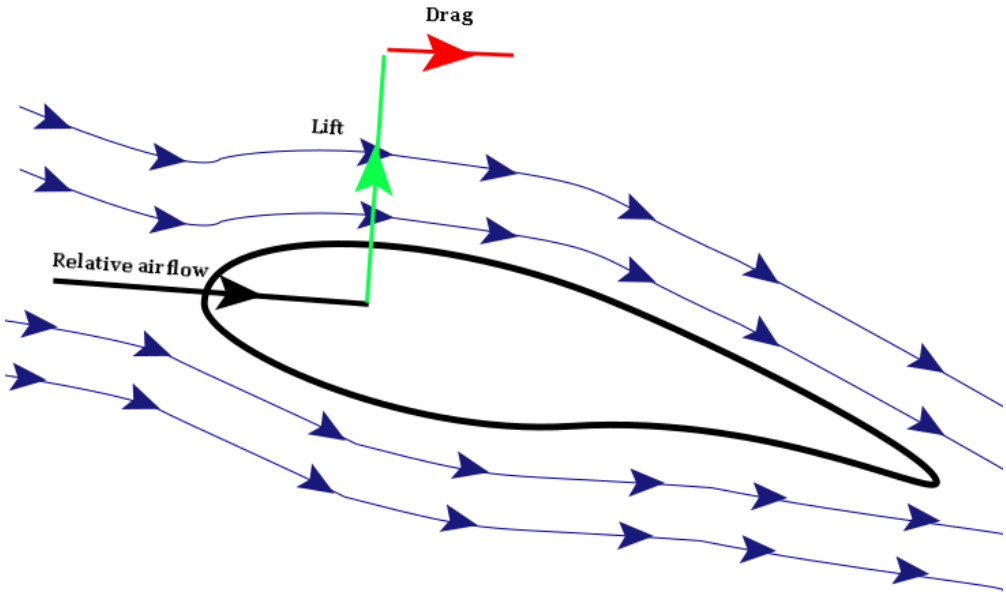

FIG. 3 Lift and drag over an airfoil [10]

The force created by the wind depends mostly on the angle that the blade creates with respect to the wind direction. A bigger angle would create a bigger lift, but also increase the drag. This angle is usually controlled through the pitch control [10] .

This way, the whole blade can rotate with respect to the hub. It means that the power that the blades take from the wind can be controlled.

2.1.2 Parts of a WECS

As said, the horizontal axis machine is the dominating design; the turbine consists of a nacelle on top of a tower. The nacelle is oriented towards the wind through a yaw mechanism, which rotates when needed.

The rotor consists of three blades coupled in a hub. As explained in 2.1.1, the blades can rotate in their own axis, in order to control the power. In modern machines, the output electrical power can also be controlled using electronics.

Coupled to the rotor is the shaft that goes into the gearbox. Out of the gearbox, there is the high-speed shaft, which goes into the generator. There are, however, Direct Drive (DD) turbines in which there is no gearbox and the hub and generator are directly coupled.

At that point, the generator converts the mechanical energy into electricity. This voltage and current are then transformed into higher voltage through a transformer. Which is usually located at the base of the tower.

There are as well, many supplementary systems that are not thoroughly explained in this work, that make the turbine work as it is supposed to. Like, the control systems, which adjust the created power and the quality of the output voltage. The yaw and pitch mechanism are part of this control systems. Most of the components can be seen in FIG. 4.

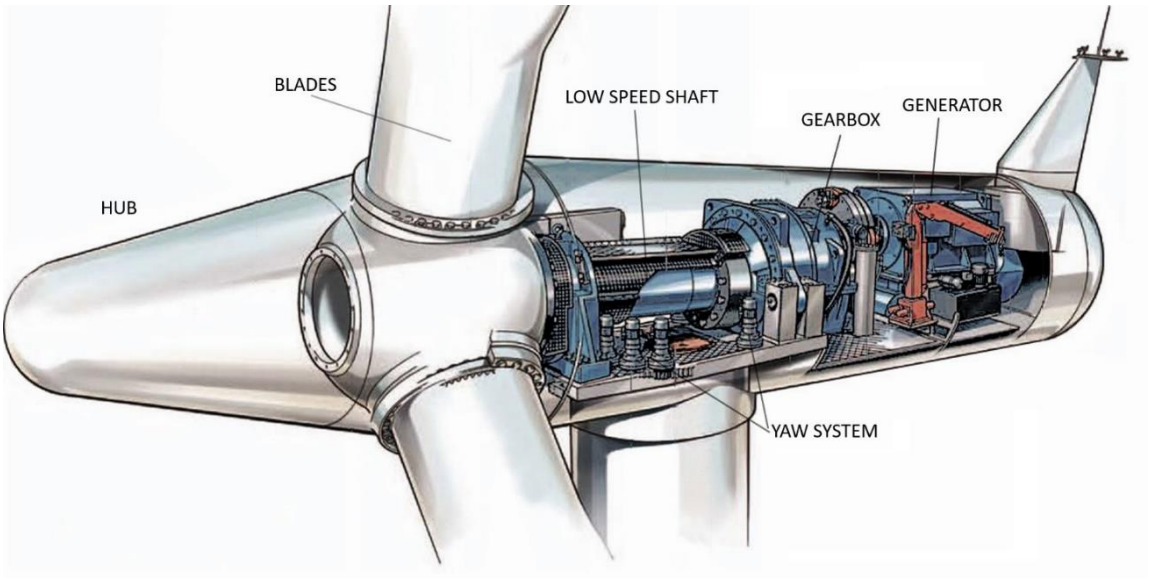

FIG. 4 Details of a nacelle [11]

2.2 Types of WECS

In this section, the different ways of classifying wind turbines are examined. First of all, it should be noted that, as previously stated, most of the commercially available turbines are based in the Danish concept that was explained in 2.1.1. Hence, almost all the turbines are Horizontal Axis Wind Turbines with three blades, and yaw mechanism.

The differences are found in the electrical and mechanical concepts of these turbines. Those are explained here. First, the different electrical topologies are explained. Later, the differences between turbines with gearbox and without are described. Finally, an explanation in generator types is made.

2.2.1 Electrical topology:

There are four main types according to this classification. The main difference between the topologies is the possibility to work at different rotational speeds. The fixed speed design works directly coupled to the grid, and the variable speed design has the possibility to change the rotational speed.

At the beginning of the development, the wind turbines were simple and directly connected to the grid. This way the generator could only rotate at the speed determined by the grid's frequency, the gear ratio and its own design.

In contrast, the flexible topology makes the machine capable of varying the rotational speed at different wind speeds, achieving this way maximum aerodynamic efficiency for all the range of operation. The tip speed ratio λ is kept constant. This tip speed ratio is the ratio between the wind speed and the translational speed of the tip. The concept is further explained later as a formula in section 3.1.

Both types need some kind of power control. It can be passive, stall controlled, or active, pitch controlled. The stall control consists on fixed angle blades, which are designed to lose power when a certain wind speed is exceeded. It is simple and robust but not efficient or consistent, because it varies with air density or turbulences.

In the pitch control, the angle at which the blades are attached to the hub can be changed. This means the power output of the blade can be adjusted to the wind speeds to follow the curve of maximum power of the turbine. It adds complexity to the turbine, but it is used anyway in almost all the modern turbines.

In FIG. 5 the power curve of an eight MW wind turbine with pitch control can be seen. The pitch control maximizes the power input at lower wind speeds turning the blade towards the wind. At high wind speeds, the blade is turned out of the wind and the power is constant. After 24 m /s, the turbine is stopped for security reasons.

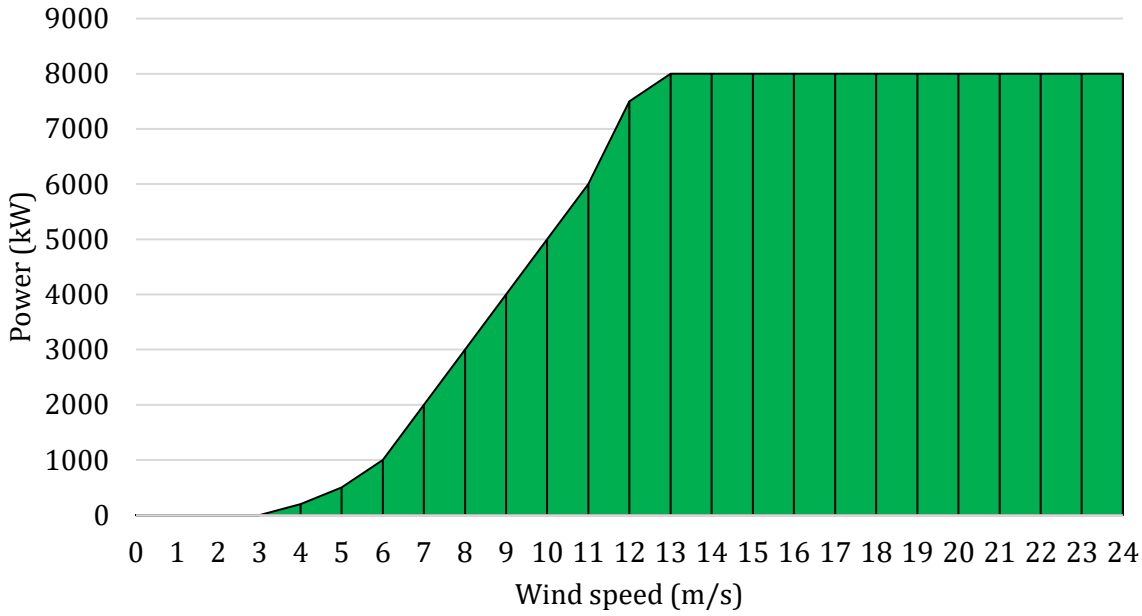

FIG. 5 Power curve of a wind turbine [5]

Considering all those, the different electrical concepts are further explained.

Type I Turbine:

This is the simplest design, and denotes the fixed speed turbine with a Squirrel Cage Induction Generator, or SCIG, connected directly to the grid via a transformer. Since the SCIG needs reactive power from the grid, a capacitor bank is added. A soft starter is used to smoothen the connection when the machine starts working; all the elements are in FIG. 6.

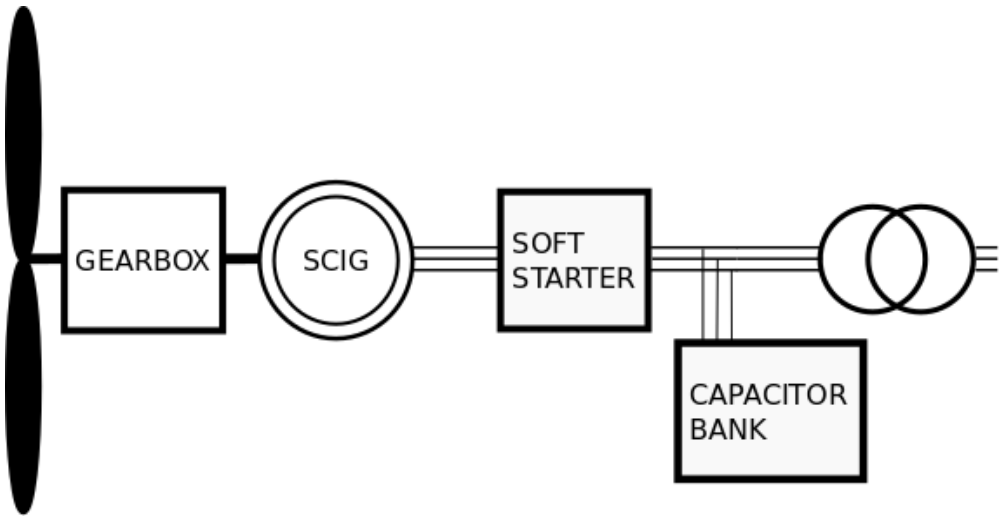

FIG. 6 Type I WECS

Type II turbine:

This kind of wind turbine, in contrast, has a limited speed variation. This is achieved through the variation of the generator rotor resistor. It is then connected directly to the grid. The Wound Rotor Induction Generator (WRIG) allows a variable slip in a narrow range, due to the variable rotor resistance.

This concept still needs a soft-starter and a reactive compensator. It is an improvement of the previous model, which allows to variate the wind speed in a narrow range around the point of operation. The slip power is dissipated in the resistor as losses. The whole configuration is shown in FIG. 7.

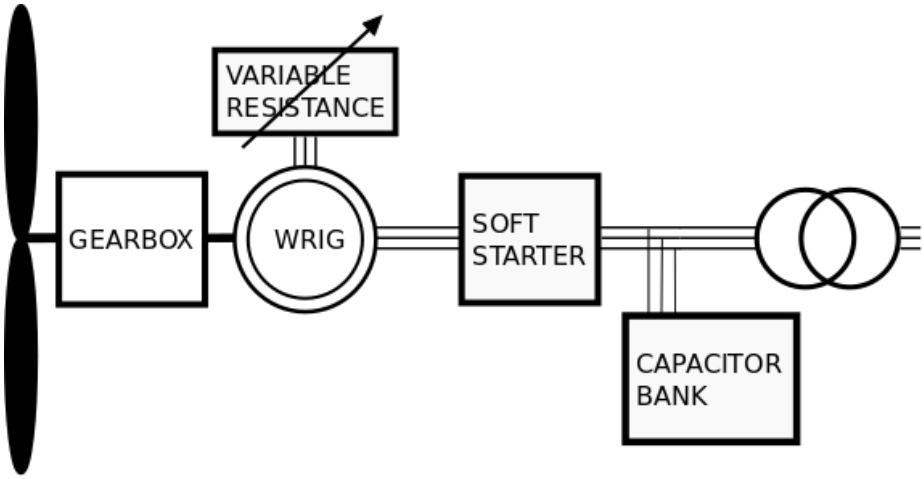

FIG. 7 Type II WECS

Type III turbine:

In this concept, a Doubly Fed Induction Generator (DFIG) has a partial-scale frequency converter connected to the rotor, as in FIG. 8. This way, the converter is able to control the speed of the generator from around -40% to +30% of the synchronous speed of the machine. It also has no need of soft-starter or capacitor bank.

Due to its flexible and economical design this kind of turbine was the most installed model in the last years [2] . It is still the most common design, mostly in onshore turbines. The modern projects, however, use the design explained in the next section.

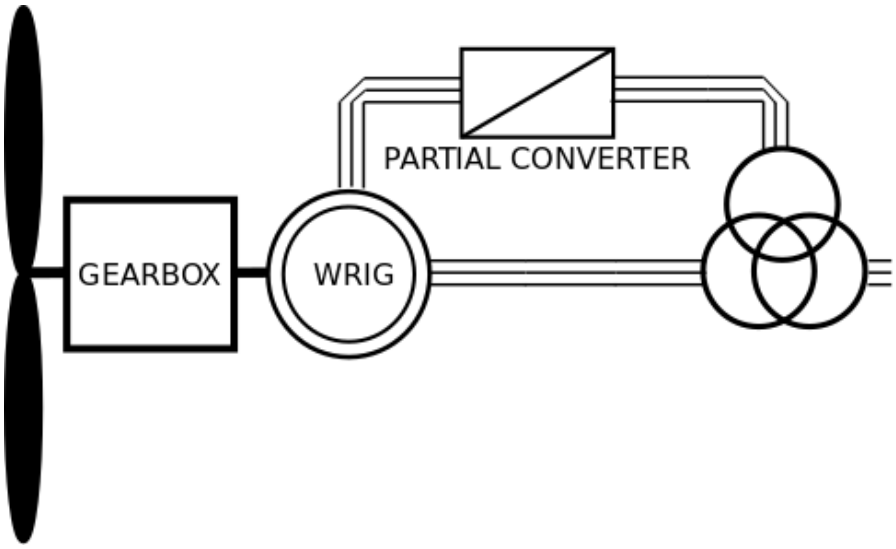

FIG. 8 Type III WECS

Type IV Turbine:

This configuration is based on the connection of a full-scale converter between the generator and the transformer, as it is presented in FIG. 9. Thus, it is able to work in very different wind speeds and to control the generation of the active and reactive power that are fed into the grid. Although the losses in the converter are summed, the overall performance is better than in previous concepts.

The generator connected to this converter can be both electrically excited or magnetically excited, that is, a Wound Rotor Synchronous Generator (WRSG) or Permanent Magnet Synchronous Generator (PMSG). There are also turbines with this design without a gearbox. Further detail on this topic is given on 2.2.2.

This is the most common topology nowadays, since it is the most flexible one and allows the most power to be extracted from the wind. The extra costs of the converter are then balanced out.

This is also the design used later in the simulation that is part of this work, as is explained in section 5.3.

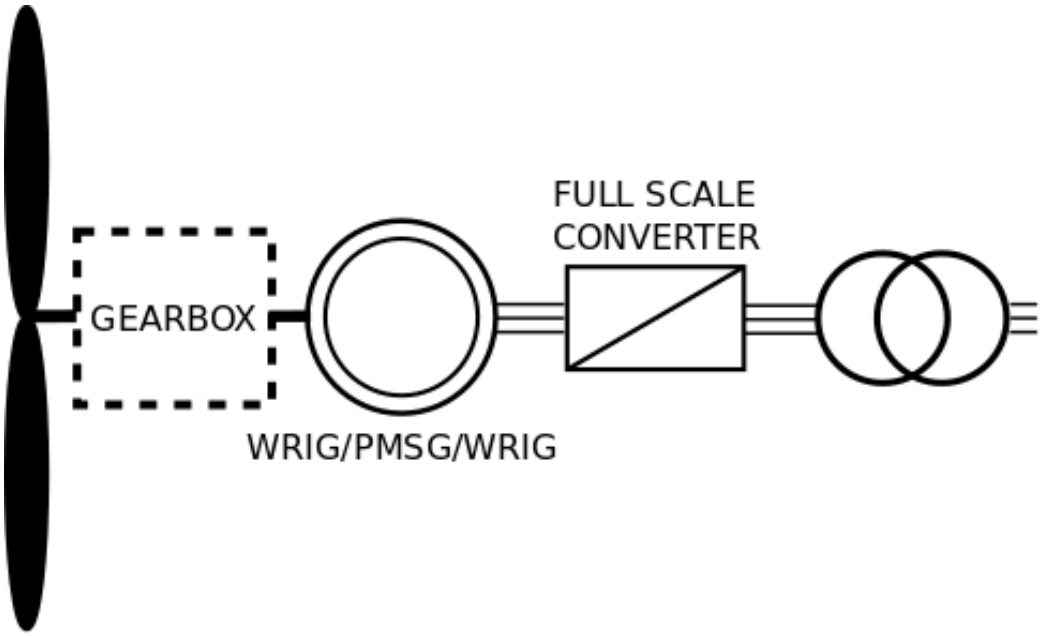

FIG. 9 Type IV WECS

2.2.2 Gearbox or Direct Drive:

In FIG. 10 [2] it can be seen that most of the currently installed turbines are equipped with a gearbox. Its function is simple, to step up the rotational speed of the input shaft that comes from the hub.

There exists, however, the option of creating a turbine system without a gearbox. There are arguments for and against this option.

Geared turbines have about 10 % lower manufacturing costs [13] mainly because the generator needs less material. Thus, the installation is simpler and less expensive. The gearbox, however, is the main failure point of this kind of design, and usually has to be replaced after a certain operation time of around 10 years.

Direct drive designs, on the other hand, need big and heavy generators. Hence, the installation of this kind of turbines is more complex. The efficiency however, is improved and the maintenance costs lowered. This can be a great advantage for offshore installations with difficult access. In addition, the design of the drive train is greatly simplified.

Considering both sides, there is no clear choice. The manufacturers usually have both designs available. As stated in [14] the use of PMSG and direct drive design is interesting in means of lower maintenance and the use of a full converter. As can be deduced form FIG. 10, the DD are becoming more common in the market. Hence, this is the option chosen for the conventional design chosen in this work.

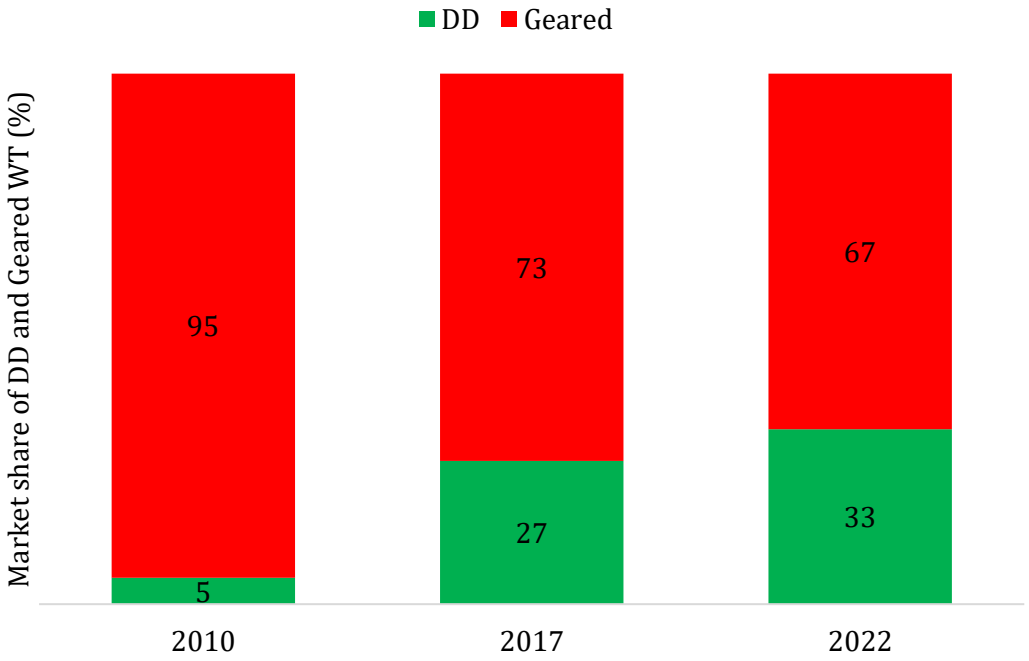

FIG. 10 Market share of DD turbines in 2010, 2017 and 2022 (predicted) [13]

2.3 Generator types

As it was explained in 2.1, there are different possibilities in the choice of the electric system of a turbine, mainly in the generator. The main difference can be made between synchronous and asynchronous machines.

2.3.1 Asynchronous generators

Induction generators are robust, mechanically simple and cheap. The main drawback is that the stator needs reactive power to magnetize the rotor. In this case, when the stator is fed by an AC voltage it creates a variable magnetic field. This magnetic field induces a variable current in the rotor, which at the same time creates a magnetic field that induces currents in the stator when it rotates at a speed higher than the synchronous speed. The slip is the difference between the synchronous speed and the actual speed.

SCIG, Squirrel Cage Induction Generator

In this configuration, the rotor is made by copper bars and two closing rings are attached at both sides, which create a short-circuited structure. It is used in fixed-speed turbines, because the speed can only change a low percentage around the synchronous speed.

As it was stated before, the soft-starter mechanism is necessary in this case, because the SCIG has a huge current when connected to the grid and with fluctuations on the input torque.

It needs reactive power as well to magnetize the stator, what causes a low power factor. Therefore, a power factor compensator in form of capacitor bank or STATCOM is needed.

WRIG, Wound Rotor Induction Generator

In this case, the electrical characteristics of the rotor can be controlled from outside by using power electronics. In this connection, the slip and therefore the speed can be limitedly controlled.

Usually the control is made through slip rings, but there are designs where the connection is made wireless. It is more controllable that the SCIG, but the need for connection slip rings makes it less robust and more expensive.

DFIG, Double Fed Induction Generator

This is the dominant concept on the market, a WRIG with the stator directly connected to the grid and the rotor connected through a bidirectional back-to-back power electronics converter.

It allows a large operation range. The converter controls the speed and the behavior of the generator injecting a current in the rotor with variable frequency. In an over synchronous situation, power is fed from the rotor to the grid. In sub synchronous operation, it flows the other way around.

This topology has many advantages. It allows controlling reactive power. The size of the converter is selected based in the speed range needed to achieve. Hence, a wider range requires a bigger converter to manage the power needs. The main disadvantage is the inevitable need of slip rings.

2.3.2 Synchronous generators

This kind of design is more expensive and mechanically complicated than the induction ones, but there is no need for a magnetizing current. Briefly explained, there is a rotating magnetic field created by the rotor. This can be done with permanent magnets, in the case of PMSG, or electric excitation, in the case of WRSG. This field induces a current in the stator that is the output of the generator.

This kind of machines are usually connected through a converter. This converter acts as a protection, by not feeding directly to the grid the variation in power created by the wind. It also allows full control over the active and reactive powers. As well as variable speed working range.

In direct drive turbines, this machine is used. The hub of a WECS turns at 9-20 rpm. This speed is quite low and in order to create a good voltage a high number of poles is needed. Thus, the radius of the machine is much bigger making it heavy and expensive to produce.

WRSG, Wound Rotor Synchronous Generator:

This design is the most used worldwide to generate electricity. In the wind industry, however, it has not been used until recent time due to complexity and the need to adapt to grid regulations. Because if connected directly to the grid it needs to rotate at the rotational frequency of the grid. Development in power electronics has made possible to create full-scale converters that manage the whole power.

The rotor winding is excited with DC current, using brushes connected to the rotor or using a brushless exciter in the rotor. In the second option, an AC current is induced in the rotor and this is then rectified to obtain DC. This makes it more complex and efficient at the same time. It is usually used in big generators.

The rotational DC current creates a rotating magnetic field. This field induces a current and voltage in the stator. These have a frequency proportional to the rotational speed of

the turbine. Using the converter, this variable frequency voltage is converted to a voltage with the grid frequency.

This design allows the design of turbines without a gearbox, as can be seen in the portfolio of some manufacturers.

PMSG, Permanent Magnet Synchronous Generator:

In this design, the excitation is made through permanent magnets, which are usually located in the rotor, thus creating a rotational magnetic field. This kind of self-excitation allows them to be more compact and very efficient. They do not have needs for slip rings or any other excitation system.

As well as the other synchronous generators the PMSG also have the need of a converter to control the output frequency and voltage. The materials used to make the magnets are sensitive to temperature changes that could make them lose their magnetic properties. In addition, these materials are prone to speculations and the price can suffer significant variations.

2.3.3 Special designs:

There are also less common designs that are being considered to be used in the future.

High voltage generator:

The output voltage level of the most common designs is about 690 V. This voltage level requires a transformer to be installed in the wind turbine in order to step up the voltage for transport and distribution. This way the current is lowered and so are the losses.

In this design, the output voltage is made much larger in order to avoid, if possible, the installation of a transformer. There are many disadvantages, such as more complex protections systems, more expensive machines and converters and the performance in long term is unknown.

Superconducting Generators:

As stated before, the application of superconducting materials to the generator could be a great solution for powerful turbines. The better conductivity means less section for conductors, thereby saving volume and weight. The overall efficiency of the machine is also high.

The main drawback of this kind of design is the need of very low temperatures and the cooling system. Therefore, it is only interesting for large power ratings of around 10 MW

or higher, in which the efficiency of the superconducting material compensates the cooling system. This way it can be as efficient as a PMSG. **Fehler! Verweisquelle konnte nicht gefunden werden.**[15]

Anyhow, the price of the superconducting material is still very expensive compared to conventional copper. The 2nd generation high temperature superconductors have a very promising performance but still a large cost.

3 Conventional Turbine Design

In this section, the final choices for the conventional model are made. The generator, converter and turbine topology are chosen. The theoretical design of the turbine and generator are made as well.

The most common topology for wind application is the variable speed wind turbine with a full-scale converter, the type IV turbine. The PMSG is chosen, because it does not need slip rings and it is a common choice in the state of the art turbines [2] . It can be seen in FIG. 11.

The converters are chosen to be an AC/DC and DC/AC converter. Thus, a rectifier is used to rectify the voltage coming out of the PMSG generator with a variable frequency voltage, since the wind speed is variable and then an inverter is employed to create AC power at 50 Hz. The converters are further explained in 5.1.

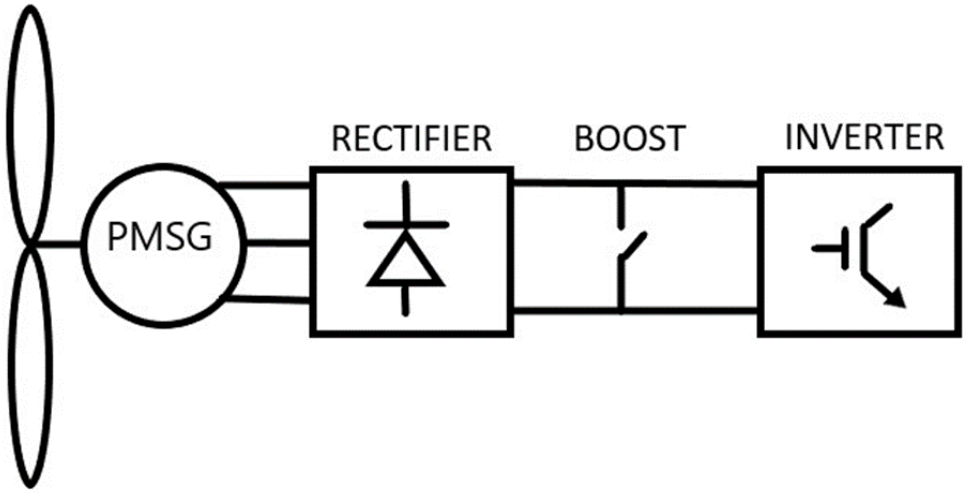

FIG. 11 Structure of the selected WECS

3.1 Turbine design

First, the power output of the generator needs to be specified. It needs to reflect the current power levels of state of the art turbines. In the manufacturers portfolio there are already 8 MW turbines, so this level of power is chosen for the conventional model [14] [15] .

Based on the power rating, the mechanical parameters of the turbine are calculated, in order to design the Simulink model. As stated first in 2.1.1, the energy of the wind E_w coming into the turbine in a period of time t is calculated as:

$$E_w = \frac{1}{2}mv^2 = \frac{1}{2}At\rho v_w^3 \tag{3.1.1}$$

Where m is the mass of the entering wind ,ρ is the density of air, v_w is the wind speed and A is the surface spanned by the blades. In the turbine this area is calculated as:

$$A = \pi R^2 \tag{3.1.2}$$

In which R is the radius of the turbine blades. The maximum mechanical energy that is converted to the rotating shaft is the wind energy multiplied by the energy conversion coefficient. c_p , which as stated before, has a maximum value of 0.59. The power coefficient of the machine describes the fraction of the wind speed captured by the turbine. This way the mechanical power out of the turbine P_m can be calculated:

$$P_m = c_p P_w = c_p \frac{1}{2}\pi\rho R^2 v_w^3 \tag{3.1.3}$$

In addition, the rotational speed of the rotor is then calculated as a function of the tip speed ratio. In order not to make the tip speed too large, an optimal tip speed ratio $\lambda_{opt} = 8.1$ [2] is chosen [2].

$$\omega_{turb} = \frac{\lambda_{opt} v_w}{R} \tag{3.1.4}$$

For this project, a turbine with an electric rated power $S_t = 8\ MVA$ is chosen, reflecting the trend of the industry of building bigger turbines for offshore locations. According to this, the mechanical power that the turbine has to be able to take out of the wind is $P_m = 8\ MW$, without having into account the mechanical efficiency. Only the power coefficient is used with a maximum value of $c_{pMAX} = 0.51$. Using this value and the previous formulas, the rated power and the rated wind speed, the radius of the turbine is calculated. The other mechanical parameters are chosen using the turbine in [21] as reference.

Table 1 Mechanical parameters of the designed turbine

Parameter	Unit	Value
Rated maximum power coefficient c_{pMAX}		*0.51*
Air density ρ	Kg/m^3	1.225
Rated wind speed v_w	m/s	*12*

Turbine radius, blade length R	m	72.037
Optimal blade tip speed ratio λ		8.1
Turbine rotational speed ω_{turb}	rad/s	1.35
Turbine rotational speed n_{turb}	rpm	12.88

3.2 Generator design

The next step is to calculate the electrical parameters of the generator. The chosen generator is a PMSG. There is no gearbox so the generator is directly coupled to the turbine hub. As stated in 2.2.2 the lack of a gearbox has some advantages. The PMSG is mechanically simpler and has a high efficiency. No gearbox means less losses and less maintenance [14] [21] .

However, the lack of gearbox makes the speed at the generator quite low, so a large number of poles is required. This is made in order to achieve a high enough frequency and avoid the losses in the magnetic core **Fehler! Verweisquelle konnte nicht gefunden werden.**. Besides, the radius of the generator is large compared with a high-speed machine with a gearbox and less poles.

According to [27] the parameters of the turbine are calculated. The goal is to obtain the phase resistance R_s, the armature inductance L_{sm} and the flux linkage in the stator winding created by the magnets λ_m to introduce the values in the Simulink model.

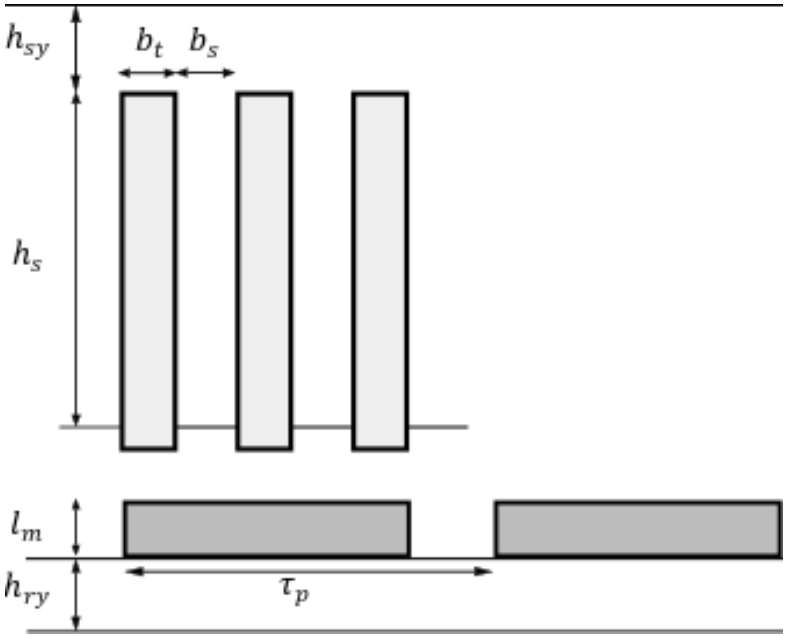

FIG. 12 Section of the PMSG

First of all, basic parameters are selected according to [14] [21] . The geometrical parameters can be seen in **Fehler! Verweisquelle konnte nicht gefunden werden.**, where the black blocks at the bottom are the permanent magnets in the rotor, and on the top are the different slots in which the active conductors are located.

Table 2 Parameters of the PMSG

Parameter (unit)	Unit	Value
Number of pole pairs N_p		80
Number of slot per pole per phase q		1
Remnant magnetic flux of the magnets B_{rm}	T	1.2
Number of phases m		3
Stator radius r_s	m	3
Diameter of the air gap D_s	m	5.86
Height of the stator yoke h_{sy}	mm	40
Height of the rotor yoke h_{ry}	mm	40
Magnet height lm	mm	20
Air gap g	mm	10
Slot filling factor k_{sfill}		0.65
Magnetic permeability of vacuum μ_0	H/m	4π exp-7
Active recoil permeability of the magnets μ_{rm}		1.05
Resistivity of copper at 120°C ρ_{Cu}	μΩm	0.025
Length of the exterior armature l_{ext}	m	0.02

Based on the parameters in Table 2 the process to calculate the rest of the values is described as follows. First, the diameter of the air gap D_s, the actual air gap g and the number of poles $2N_p$, determine the pole pitch τ_p:

$$\tau_p = \frac{2\pi\left(\frac{D_s}{2} - g\right)}{2N_p} \tag{3.2.5}$$

The magnet width b_p is related with the pole pitch τ_p by:

$$b_p = 0.7\,\tau_p \tag{3.2.6}$$

The value of 0.7 is chosen for the relative magnet width because it helps reduce the Cogging Torque. This torque is a pulsating force formed from the interaction of the permanent

magnets and the air gap permeance [36] . The width of the coil span w, is equal to the pole pitch.

The number of turns per phase N_s and the number of turns per coil N_a are calculated:

$$N_s = \frac{A_a \pi D_s}{2mI_a} \quad N_a = \frac{N_s a}{N_p q} \tag{3.2.7}$$

A_a is the stator electric loading, I_a is the electric current at rated power and a is the number of parallel branches per phase, in this case two. The missing design values are the effective air gap g_{eff} and the length of the stator l_s.These two parameters are calculated through iteration. The effective air gap is increased step by step until the magnetic field inside of the machine is equal to the one created with the magnets without causing saturation. The length of the machine is increased until the desired power rating is achieved, taking into account the losses [27]

Table 3 Results of iteration

Parameter	Value
Effective air gap g_{eff} (m)	*0.0336*
Length of the machine l_s (m)	2.34

The necessary values for the Matlab model are the magnetizing inductance L_{sm}, the phase resistance R_s, and the flux linkage of the magnets λ_m. They are calculated as follows. The magnetizing inductance L_{sm}:

$$L_{sm} = \frac{6\,\mu_0 l_s\, r_s\, (k_w N_s)^2}{N_p^2 g_{eff} \pi} \tag{3.2.8}$$

where k_w is the winding factor. It is estimated to have the value of one.

The resistance per phase, R_s:

$$Rs = \frac{\rho_{Cu}\, l_{Cus}}{2aA_{Cus}} \tag{3.2.9}$$

Where A_{Cus} is the area of the conductor, l_{Cus} is its length and a is the number of parallel branches.

$$A_{Cus} = \frac{I_a}{J_a} \tag{3.2.10}$$

With I_a is the rated current of the machine and J_a the stator current density.

$$l_{Cus} = N_s(2l_s + w\pi + 4l_{ext}) \tag{3.2.11}$$

Finally, in order to calculate the equivalent flux linkage in the stator phase winding created by the magnets λ_m [27] the next equation is used:

$$\lambda_m = \frac{\mu_0}{N_p}\frac{4}{\pi^2}\frac{\tau_p}{g_{eff}} l_s (k_w N_s)^2 \sqrt{2}\, I_a \tag{3.2.12}$$

Table 4 Results of the design process for the PMSG

Parameter	Unit	Value
Magnetizing induction of the machine L_{sm}	mH	0.13
Resistance per phase R_s	Ω	*0.019*
Equivalent flux linkage in the stator phase winding created by the magnets λ_m	Wb or T/m^2	*5.31*

4 Offshore wind farm Layouts

Offshore wind energy generation projects are usually large projects involving a large number of turbines. This is called a wind farm, like the one in in FIG. 13. The main discussion point is the possibility of using DC in the interconnection grid, unlike all the present technology connects it.

The wind turbines generate an electric energy at a certain voltage level. It is usually a low voltage level (690 V). So in order to lower transmission losses the voltage is stepped up for the collection grid. This is usually a medium voltage level (between 30-60 kV). Finally, the voltage is stepped up once more to transfer it to the shore, since the distances are usually large.

A description of the different elements and topologies is made on the following section, [17] -[19]

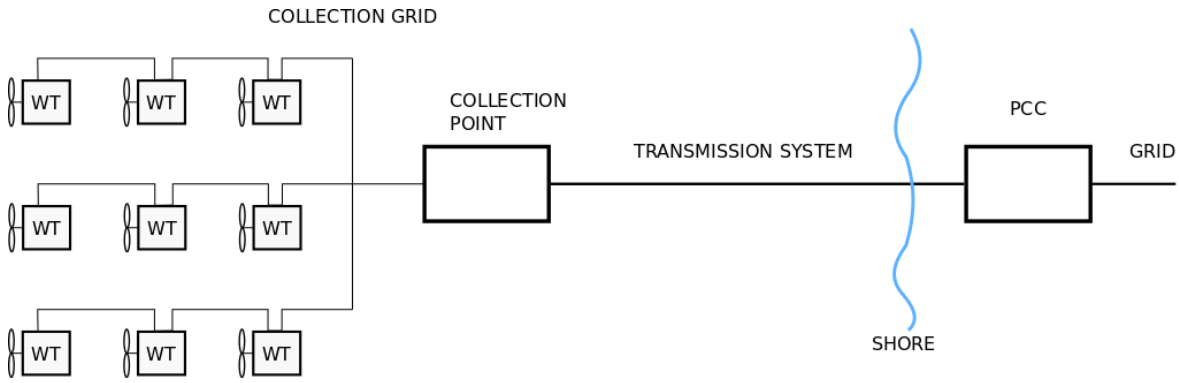

FIG. 13 General structure of an offshore wind farm

This structure consists of different elements. On the low voltage side, there are the wind turbines, with the generator, the power converter, the step-up transformer and the protection systems.

The collection grid is meant to interconnect the wind turbines and the collection point. There are different possibilities and the choice is made taking into account reliability, cost and installation. The collection is usually made in Medium Voltage Alternate Current, or MVAC. The possibility of doing it in DC is being investigated.

The collection point is an offshore substation. It collects all the lines from the turbines and steps-up the voltage for transmission, usually High Voltage such as 150 or 220 kV. The application of this structure depends on the distance to the shore and the size of the wind farm.

The transmission system is the long undersea connection to the shore. Depending on the distance, it can be done in AC or in HVDC.

Finally, the Point of Common Coupling, PCC, is where the connection to the grid is made. If the system uses HVDC, it has an inverter to create AC. There is usually a control system to ensure that the voltage, frequency and reactive power adapt to the grids requirements. There may be the need of a compensation system.

4.1 Collection grid topology

First, the different interconnection options are explained. The first classification is made based on how the interconnection of turbines is made. Without considering if it is in AC or DC. The main differences between topologies are the length of cables needed and the protection levels obtained. A compromise between cost and reliability is made.

There are many different possibilities but mostly three topologies are actually being considered [20]

4.1.1 Radial design

A number of turbines are connected in a branch, and the different branches are then connected to the collection point. The number, m, of WT connected depends on the power rating and the geographical location, but is usually between 5 and 10. In FIG. 14 there is an example.

The main advantage of this configuration is that it is the least expensive one. The cable length is the minimum needed of all designs. It also can be designed with different cable ratings. The last section is only fed from one turbine and the cable rating can be increased as the collection point is approached. This option makes the installation more complex so it is not usually used.

The reliability of the system is a clear disadvantage. A failure next to the connection point leads to the loss of a whole branch. Anyhow, this is almost the only topology used, since the main consideration point for the manufactures is the cost.

4.1.2 Dendrite or star design

In this design, the connection to the collection point is made through a central turbine. This way, the cables going to the center WT have a lower power rating than in the radial

design. The cable from the central hub is rated for the full power, as in

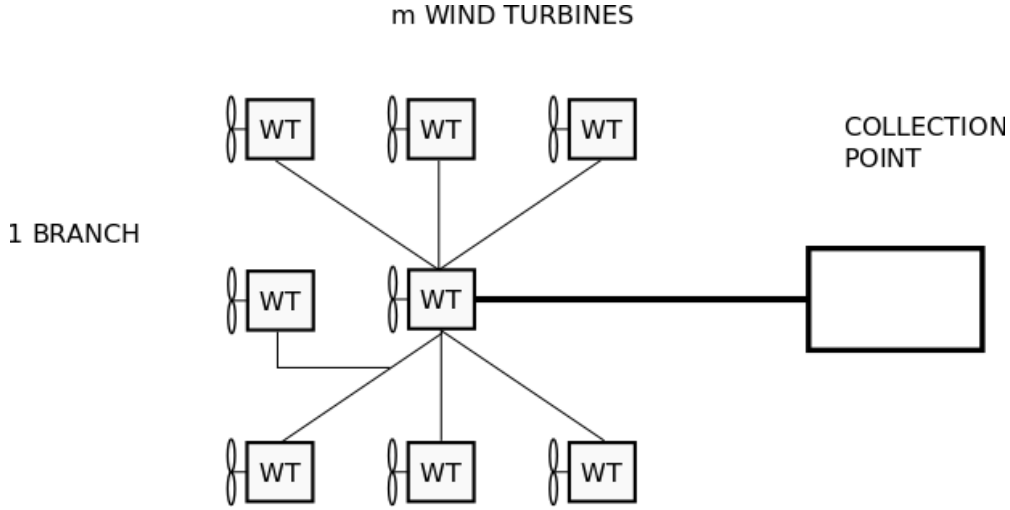

FIG. 15.

The reliability is improved since the failure of a cable would only disconnect one turbine. Except on the main feeder cable. The downside of this design is that there exists the need for costly switchgear at the central turbine. Moreover, the cable and installation uniformity is lost.

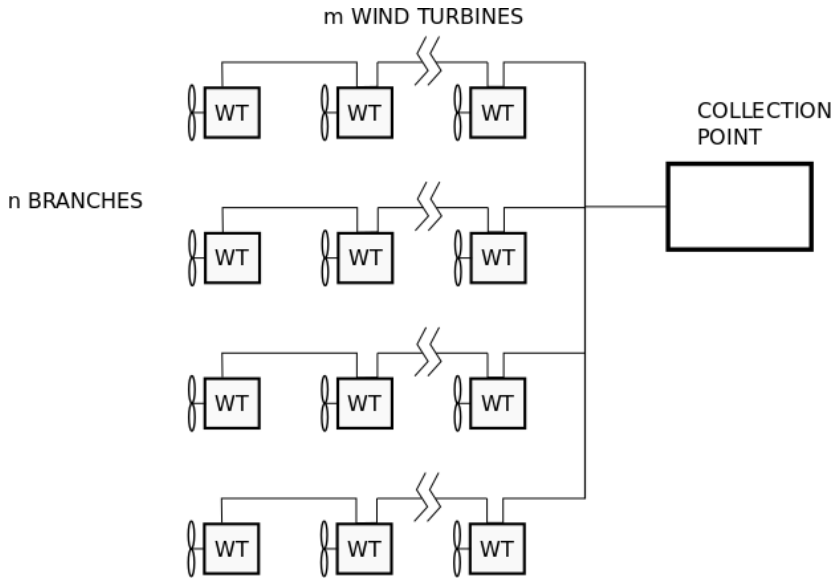

FIG. 14 Radial wind farm topology

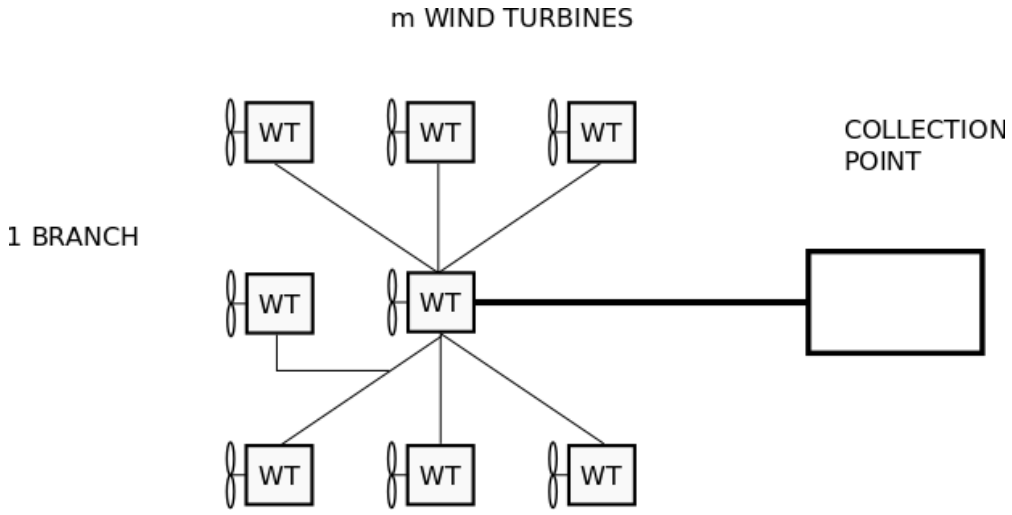

FIG. 15 Dendrite design wind farm

4.1.3 Double sided ring

This topology is an evolution of the radial one, by interconnecting the last turbines of two adjacent branches, as in FIG. 16. This way the reliability is improved. In case of a failure in an interconnection, the power can flow through the other branch.

The cable at both ends of the hub needs to be designed to transfer the power of both branches. Hence, the costs are increased.

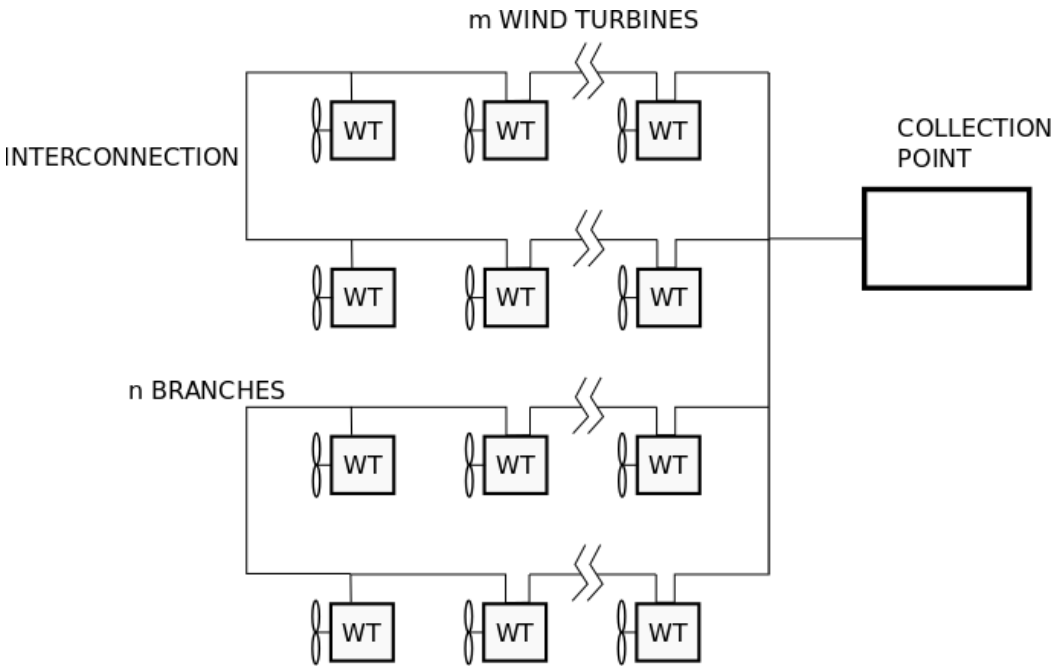

FIG. 16 Double-sided radial design wind farm.

4.2 AC wind farm grid topology

In this section, the different AC collection grid topologies are explained. AC is actually the only technology applied, since the DC collection grid option is yet a concept. It consists usually of a variable speed WECS with a step-up transformer. This energy is then collected and sent to the shore.

The main difference between the options is the usage of an offshore substation. When the distance to the shore is long, the voltage level out of the turbine system is not enough and another step-up is needed to transmit the power to the shore. It can be transferred either in AC or in DC.

4.2.1 Small AC wind farm

If the distance to the shore is short, the collection system is directly connected to the shore, as in FIG. 17. This is only feasible for farms really close to the shore, since the voltage level after the transformer at the bottom of the tower is not very high. The losses would be not economic in longer distances.

This voltage level is therefore selected to be high, between 50 to 75 kV. This calls for bigger transformers than the usual 30 to 36 kV. This is the design used in the first offshore wind farms.

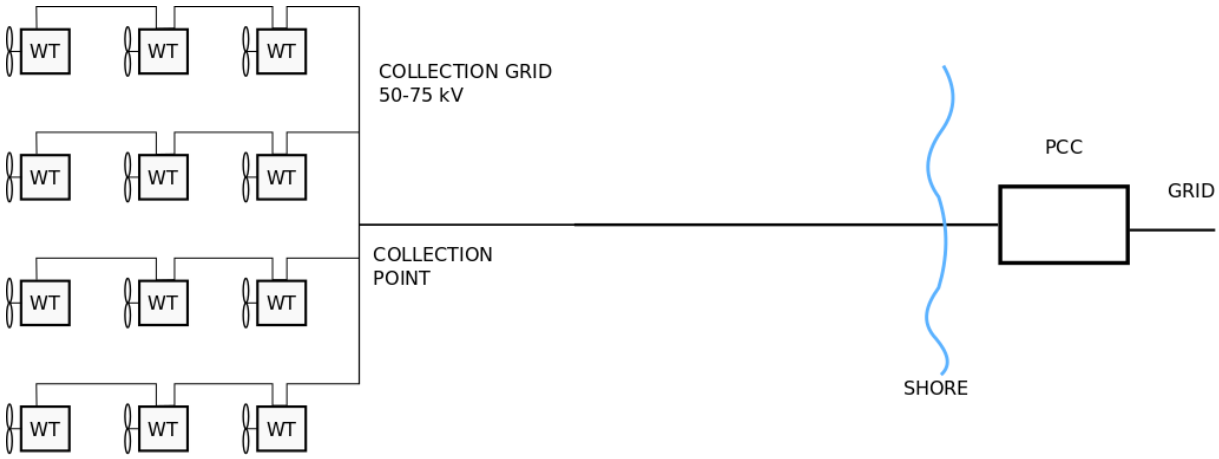

FIG. 17 Electrical connection of a small AC wind farm

4.2.2 Big AC wind farm

In this topology, the distance to the shore is longer and the number of turbines is large. It is the usual wind farm layout. An offshore substation is needed. The collection system is connected to the substation with an adjusted voltage and a step-up to a higher voltage is made, in order to transfer it to the shore.

The offshore platform is a large cost in the project and may be difficult to access in winter months in the North Sea. Therefore, attempts are being made to create a system without this need, as it is further explained in section 4.3.2.

The transmission can be made in HVAC or HVDC. The HVDC system has a higher cost, but its efficiency is higher for very long distances. At distances over 100 km, the HVDC system is preferred [19] The variation of energy production cost is shown in

FIG. 18. The two options are explained. The different options are illustrated in FIG. 19, FIG. 20 and FIG. 21.

Full AC wind farm, AC transmission system

In this case, the offshore platform is equipped with an AC step-up transformer and the needed switchgear, like in FIG. 19. The usual voltage level in the collection system is 33 kV and the transmission system works at 150 kV. In large installations, a parallel transmission is possible, and hence two transformers would be needed, like in FIG. 20. The reliability is improved this way and more power can be transported.

The advantages of the AC transmission are that the installations costs are lower than for DC transmission. However, the long distance undersea cables produce a large amount of

capacitive reactive power. The system works synchronous with the main grid and any fault transfers from one to the other.

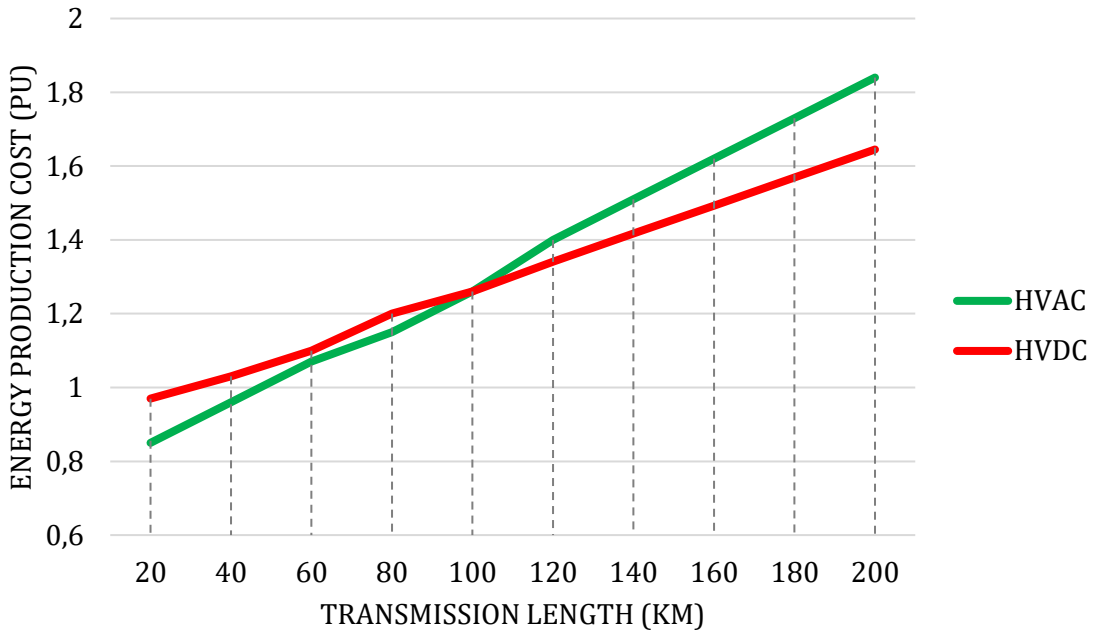

FIG. 18 Normalized production cost of wind farms as function of the transmission distance for different transmission systems [19]

Therefore, the main issue of this system is how to provide the reactive power compensation. The amount to be compensated depends on the load. There is a fixed amount that needs always to be compensated and a variable amount depending on the wind turbine generation, with a maximum under no load conditions.

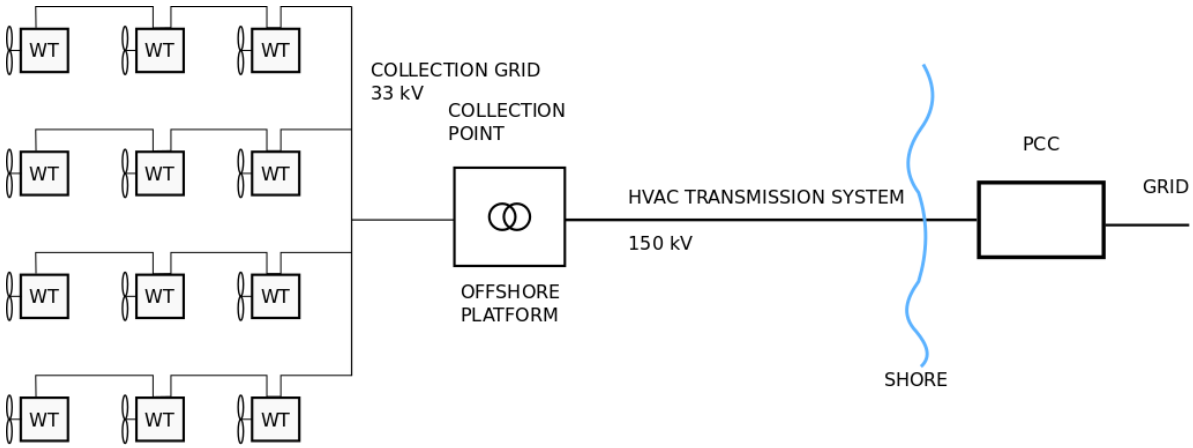

FIG. 19 Full AC wind farm

The fixed systems usually are less bulky than the variable compensators and are usually located offshore, whereas the others are located onshore [22] . The voltage level at the

PCC is controlled by both systems and the reactive power generation systems from the turbines.

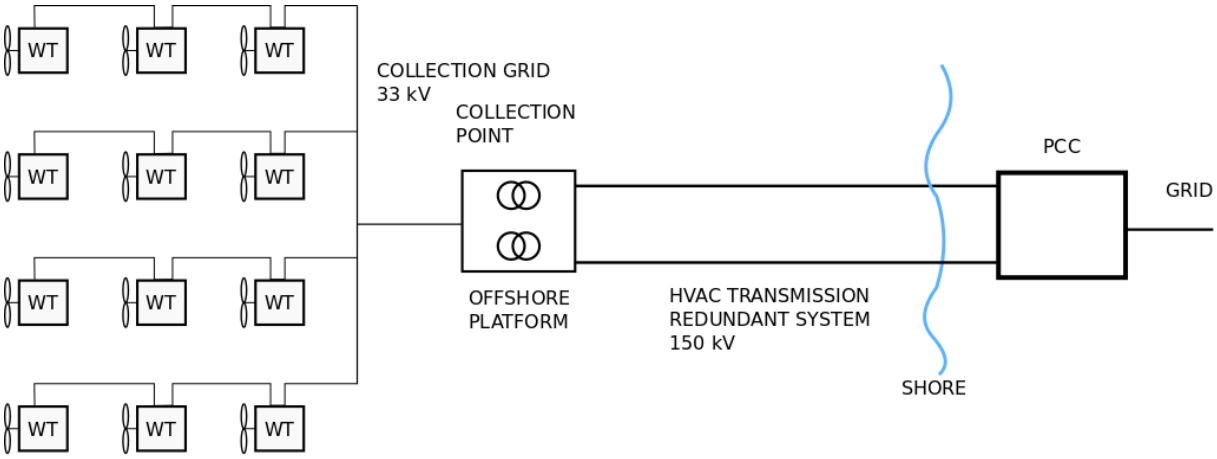

FIG. 20 AC wind farm with parallel transmission.

The AC/DC wind farm, HVDC transmission:

As explained before this kind of technology is used when the wind farm is far from the shore. AC undersea cables would need too large amounts of reactive power to work. The offshore rectifier system and the onshore inverter system are costly, but the better performance balances that out.

In addition, it allows separate frequency control of the offshore gird and the general grid, unlike the HVAC. Thus, performance and reliability of both systems is improved. The system is based on Voltage Source Converters, VSC. It allows the control of active and reactive power. Hence, the system has the capability of black-start when disconnected. The scheme is shown in FIG. 21.

The VSC are based on IGBTs with a switching frequency between 1.3 kHz and 2 kHz. [20] First, the voltage level of the collection system is raised with a common transformer and then rectified to DC. More information about converters can be found in chapter 5.

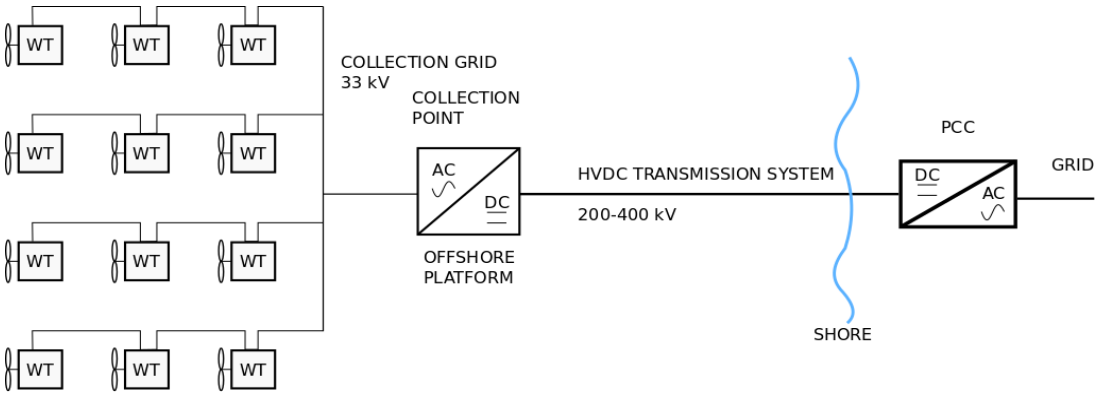

FIG. 21 AC wind farm with HVDC transmission to shore,

4.3 DC wind farms

In this case, the collection grid of the wind farm works in DC, in contrast to the conventional model. The turbine can generate AC and then rectify the voltage to DC. There are also concepts based in DC generators.

The technology used in this farm already exists, but there is no real case. There has been a lot of investigation in recent years [17] -[19] [23] **Fehler! Verweisquelle konnte nicht gefunden werden.**[25] .

With the use of DC, the need of heavy and bulky AC transformers in the towers can be avoided. The access to offshore wind farms is difficult in case of a failure, because usually the whole transformer needs to be replaced.

In AC wind farms, all the voltages out of the different turbines need to be synchronized with the same frequency. Therefore, there is a need for interconnected control systems. In DC there is no need for that and each turbine can have independent control and maximum power output.

The AC undersea cables have high capacitance losses that need to be reduced and compensated. In DC this is heavily reduced making the collection grid more efficient. The DC cables, as well, need only two conductors instead of three. Thus, saving weight and installation costs. Further explanation about cables is made in section 4.4.

Moreover, in the series wind farm design, the use of the offshore collection point can be avoided. This means a large reduction of costs. The challenges are also substantial, since the technology is still in development. The DC-DC converters are still in development or have too high losses for high voltage levels. This concept is further explained in section 4.3.2.

The main problem with the concept of DC grids is the need of some way to step-up the voltage levels. In AC it is done easily with transformers but in this case DC-DC converters are needed. There was no need of high voltage and high power converters before, so its development is a key for this technology. The converters are further explained in section 5.2.

Another critical issue with DC wind farms is the protection system. The switches for AC high voltage and current are standardized and a proven technology. But for DC there was no need in the past. The DC current does not become zero in every cycle like in AC, therefore, is more difficult to cut it. This is an important topic, but it is not in the scope of this work.

4.3.1 Parallel DC

This design is similar to the conventional radial wind farm. The difference is that the collection grid works in DC. There are no transformers and instead DC-DC converters are used. The voltage levels are similar to those in AC.

The output voltage levels are LV, usually 690 V. This is not enough to use in the collection system, therefore a step-up converter is needed in order to feed the voltage to the collection grid. The voltage is then raised again in the collection point to be transmitted to shore. The transmission system would then be a HVDC. Only that one step-up is made here, instead of a rectification. The transformer in the offshore substation is then unnecessary. The topology is shown in FIG. 22.

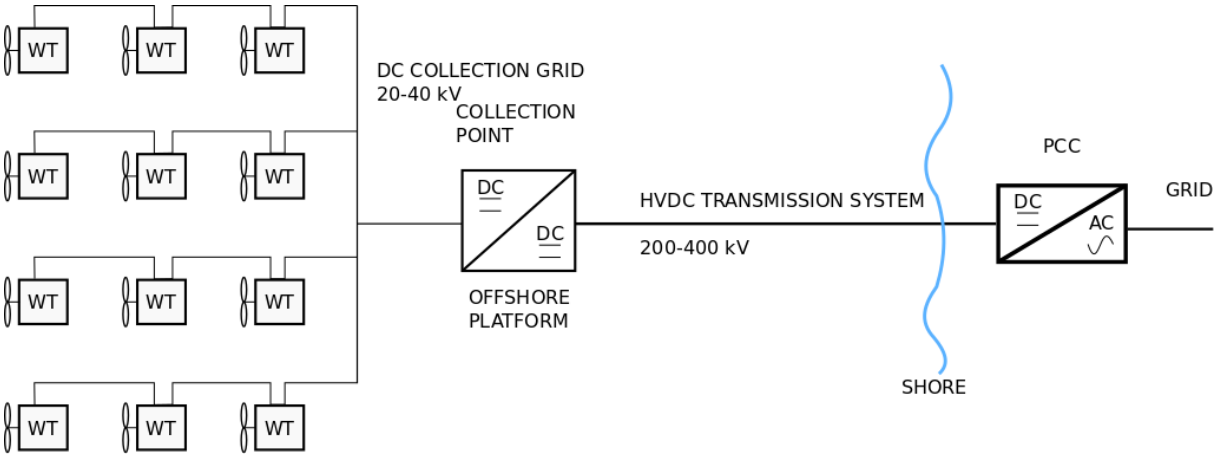

FIG. 22 DC wind farm

There is another option, as shown in *FIG. 23*. Instead of using a step-up converter in each turbine, a group of turbines shares one converter. This would be also an option in AC connections with shared transformers, but since the cost of DC-DC converters is higher than for AC transformers the question is considered in this section.

This way, less converters are needed. The losses in the collection grid are higher and another platform may be needed, unless the converter is located in a turbine. This option is therefore deemed too costly **Fehler! Verweisquelle konnte nicht gefunden werden.**.

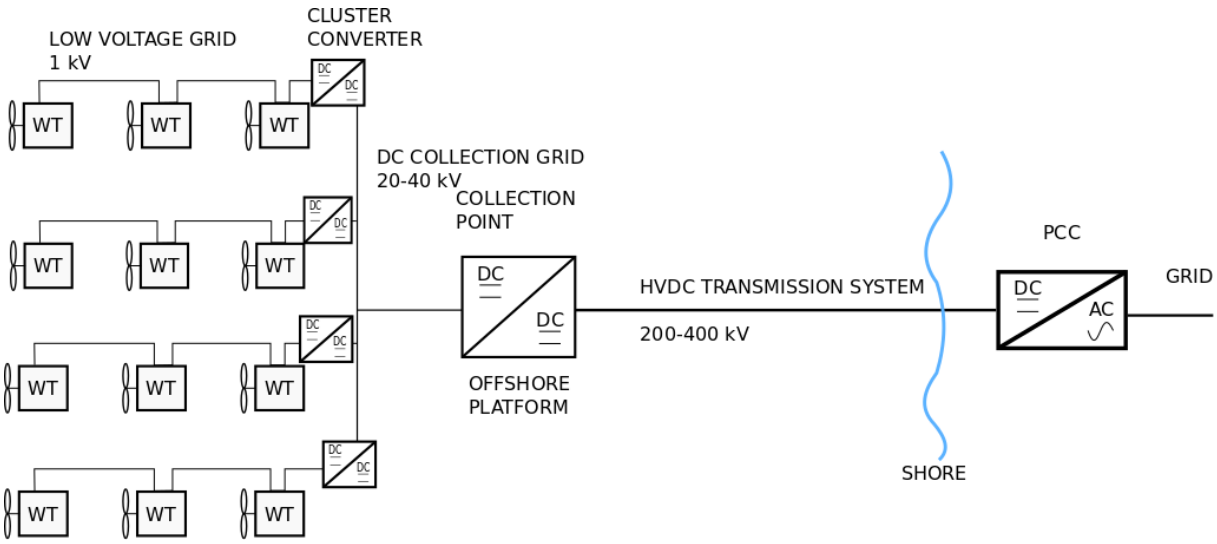

FIG. 23 Shared converter DC wind farm

4.3.2 Series DC wind farm:

In this case, a group of wind turbines is connected in series in order to add their voltage levels. This high voltage level is then transmitted directly to shore, avoiding the use of an offshore substation.

The savings when the use of a substation is avoided are significant, up to 120kEuro/MW, [19] Thus, the economics is the reason why this concept is studied, but the challenges are substantial.

From the system in FIG. 24, it can be deduced that the sum of all the voltages of a branch equals the voltage out of it, in steady state. The voltage out of each turbine cannot be controlled from the HVDC transmission system.

The output power of all the wind turbines in the branch is set by the machine with the lowest production. The current going out of this turbine limits the current to the other turbines, since the current is the same in a series connection.

In the worst case scenario, a wind turbine is not producing and is disconnected by the control system. The rest need to create a higher voltage in order to achieve the transmission voltage. Therefore, the output voltage of each machine needs to be over-rated, compared to a conventional design [19]

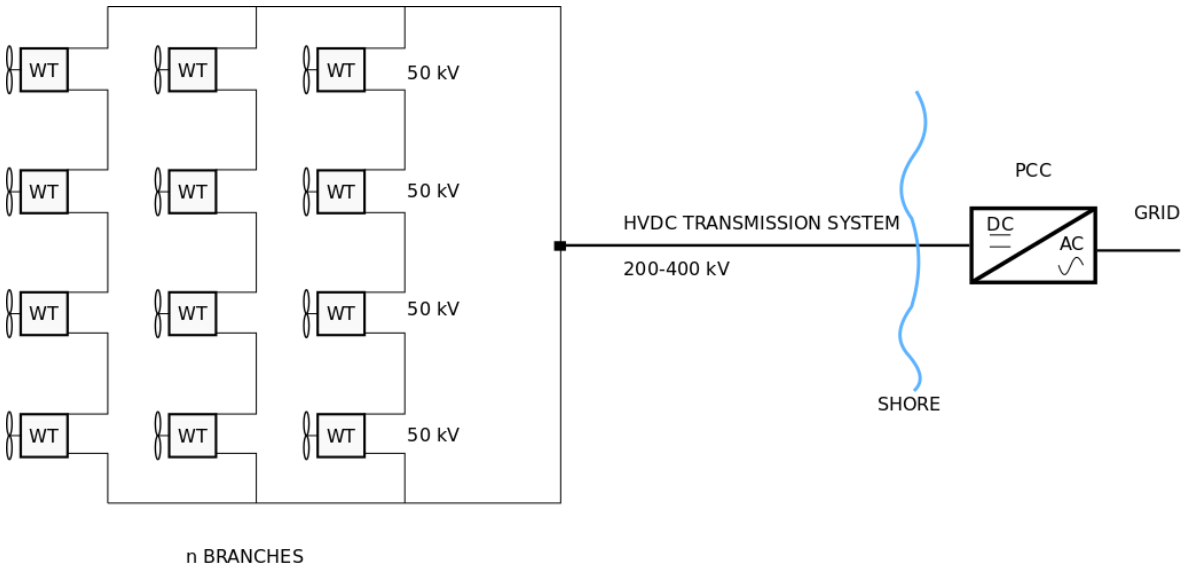

FIG. 24 Series DC wind farm

The potential that each of the turbines needs to withstand is higher in this design. The output components of the wind turbine that are connected to the other turbines need to tolerate the whole voltage of the branch. This calls for more expensive protection devices. The protection system has the capability to short circuit the output of the turbine to avoid the loss of the whole branch, as the example in FIG. 25 shows.

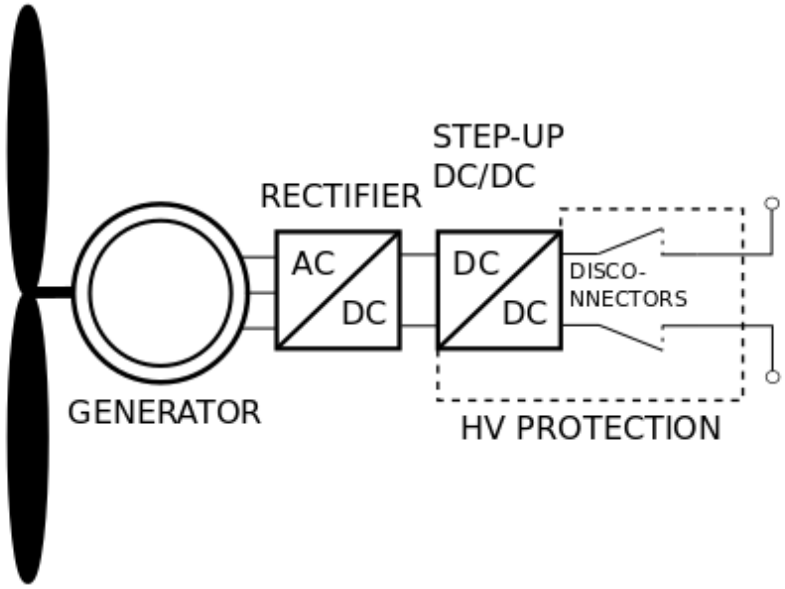

FIG. 25 WECS design for a series connected wind farm

Since the challenges this kind of connections represents are complex, it is deemed impossible to include this kind of design on this work.

4.4 Cables for offshore wind farms

In this section, the cables that are used for the collection grid of wind farms are described. Their electrical characteristics are explained as well. This parameters are used later in chapter 6 for the simulation of the wind farms.

These cables are designed for medium voltage collection grids. Since it is located offshore, they are buried at the seabed. There are also cables for high voltage transmission, but are not considered for this work.

The conventional cables are three-core cables. Each individual conductor consists of the actual copper conductor, the inner and outer conductive layers to control the fields and the high-voltage insulation, usually made from cross-linked polyethylene (XLPE). The core is surrounded by galvanized steel wires which protect the cable against mechanical damage. The general structure can be seen in FIG. 26.

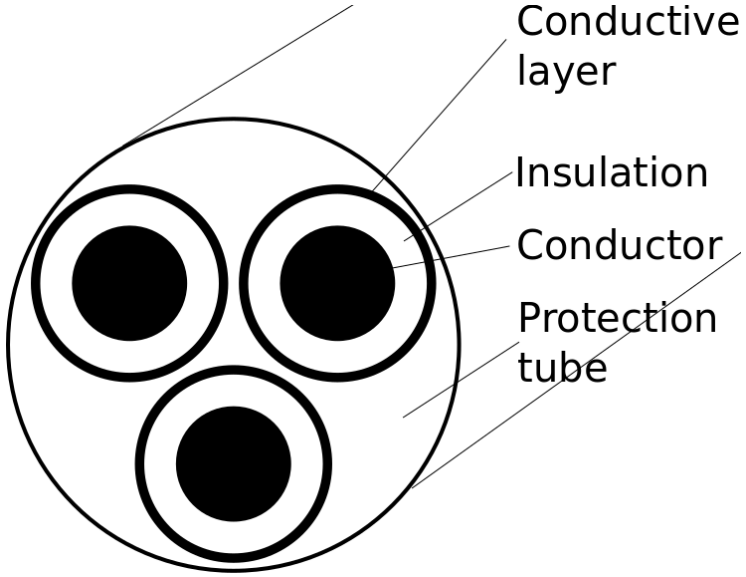

FIG. 26 Section of a three core cable

The design of cables is different for AC or DC systems. Instead of using three core cables, the DC system uses two core cables, one for the positive and the other one for the negative. The cost is therefore less.

In addition, the DC system does not create skin effect on the conductor. The skin effect is created in AC systems due to frequency. The current is mostly transmitted on the outside of the conductor due to this effect. In DC cables, therefore, the resistance is lower than in AC cables. In addition, the same cable can transport more power in DC than in AC with the same voltage. The AC cable needs reactive current in order to charge the capacitance of

the cable. This current takes part of the conduction section and therefore the active current is less than for DC systems that do not need this reactive power.

The cables are dimensioned depending on the current they can carry. The electric parameters of cables can be found in the portfolio of manufacturers, like in [39] In the case of MV cables, the same cable can be used for AC and DC, since both systems have the same power rating.

The cable segments in AC are usually modeled with the π-link model, as shown in FIG. 27. The cable parameters are introduced in the model and the simulation in steady state is quite accurate. When simulating high frequency events, however, other models have to be considered. These events include connections and disconnections to the grid as well as faults [37] . For this work, that does not involve any of that, with this kind of model is enough.

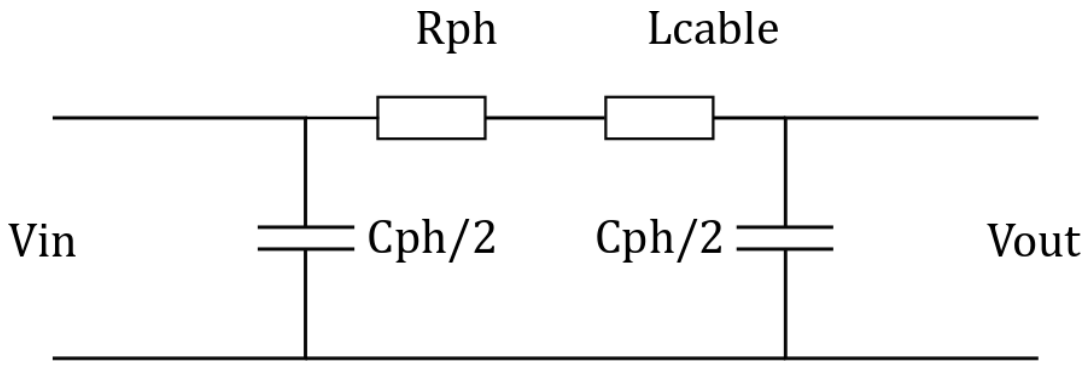

FIG. 27 Pi model of a transmission line

The resistance of one phase is the resistivity of copper ρ divided by the cross section A and multiplied by the length of the cable l:

$$R_{ph} = \frac{\rho}{A} l \tag{4.4.1}$$

The inductance of the cable L_{cable} can be calculated using the inductance per km L_{km}:

$$L_{cable} = L_{km} l \tag{4.4.2}$$

In addition, the capacitance per phaseC_{phase} is:

$$C_{phase} = C_{km} l \tag{4.4.3}$$

In DC cables a resistive cable model can be used in steady-state analysis [38] . Only the resistance per phase is needed, calculated as in (4.4.4). Since there are two cables, the resistance of the whole cable would be two times the resistance of each section. This model is shown in FIG. 28.

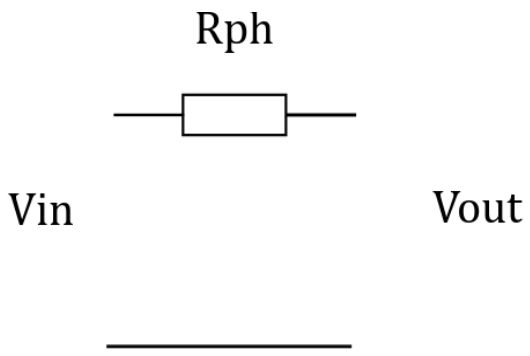

FIG. 28 Resistive cable model for a transmission line

5 Converters for WECS

In this chapter, the different electronic converters that are used in WECS are presented. First, the types that are used in AC systems and afterwards the types that can be used for DC systems. Finally, the topologies used in this thesis are described.

The converters are based on state of the art solid-state switches. Like Insulated Gate Bipolar Transistor, or IGBT, high voltage diodes or Metal-Oxide Semiconductor Field-Effect Transistor, or MOSFET. The typical characteristics and power ratings are presented in Table 5.

Table 5 Characteristics of typical semiconductor power switches [28]

Device	Maximum voltage (kV)	Maximum current (A)	Maximum frequency (kHz)
DIODE	5	5000	1
IGBT	1.2	400	20
MOSFET	1	4.7	100

5.1 Converter for AC systems

As explained in chapter 3, the technology chosen in this work is a variable speed design with a PMSG. The generator is connected to an AC-DC-AC converter. The voltage is generated with a variable frequency out of the generator and then rectified. The DC voltage is then inverted again. The voltage is controlled to have 50 Hz and is fed to the transformer and the collection grid.

The converter is a Voltage Source Converter. In this kind of converter six switches, usually IGBTs are connected to the three phases of the generator, like in FIG. 29. The switches are opened and closed using Power Width Modulation, PWM.

Usually, there are two VSC in a back-to-back construction. The machine side VSC is used to control the speed of the machine by electric means. The PMSG, as it was said in section 2.3.2 is excited using permanent magnets on the rotor so the only way of speed control is the control of the stator currents. The grid side converter is used to maintain the DC voltage at a constant level and to create a controlled voltage out of the device. This way the quantity of active and reactive power generated by the system can be controlled.

In order to fulfill all these requirements, the VSCs at the machine side or at the grid side are controlled differently. There are several control strategies **Fehler! Verweisquelle konnte nicht gefunden werden.**The idea of the controller is to provide vector control of the voltage and current. That means to control their magnitude and orientation.

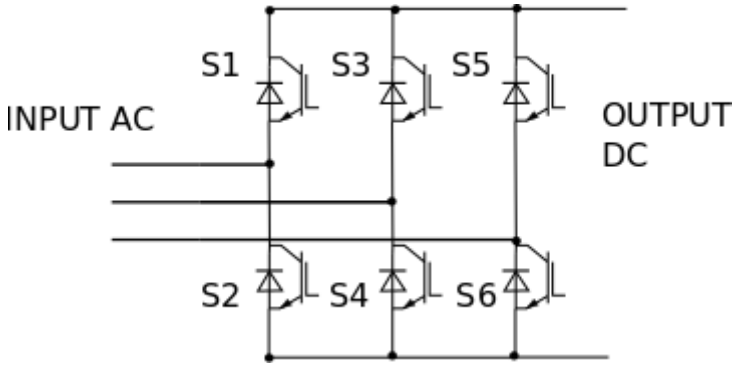

FIG. 29 Switches in a VSC converter

In this thesis however, the machine side converter is removed and instead an uncontrolled diode rectifier is used, FIG. 30. This way the efficiency is better and it can be converted into a DC system more easily. The control of the machine, however, is slower and its done instead with the control of the current made by the boost converter connected on the DC bus. The rectifier is a full wave system with two diodes for each phase and cannot be controlled.

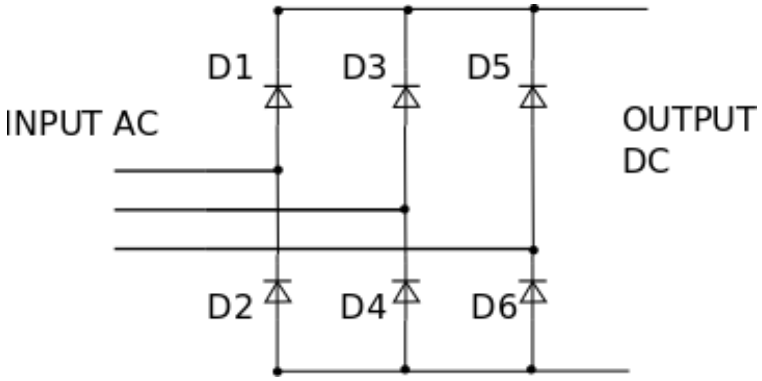

FIG. 30 Three phase uncontrolled rectifier.

5.2 Converters for DC systems

The DC wind farms that are presented on chapter 4.3 are based on the use of DC/DC converters that allow changing and controlling the voltage levels. They are equivalent to the big AC transformers and work as voltage control.

The usual applications for this kind of equipment are for low power such as Solar Energy systems, informatics and house appliances.

In the case of high power systems like wind power, just one switch cannot withstand the whole power rating ($\approx 10MW$). Therefore, a number of switches is used in parallel and

in series to share the high voltage and current. For simplicity reasons, in this work low number topologies are used.

The classification of the converters that is made here is based on the kind of electrical insulation they provide between the two steps. There are galvanically insulated converters and non-insulated. The second type use high frequency transformers to step-up the voltage.

The main application for this work is to work as step-up converters. Therefore, the most used and simplest converters are explained here. There are many other options [30]

5.2.1 Non-insulated converter

In this kind of converter there is no need for a transformer, the step-up function is made with use of inductances and capacitances.

Boost converter

It is the most basic converter and can be used to obtain a step up of 1 to 5 times the input voltage. The topology can be seen in FIG. 31. When the switch is in on state, the energy stored in the capacitor is released. When the switch is off the diode is conducting and the output voltage is the sum of the input and the voltage across the inductance. This is repeated every cycle.

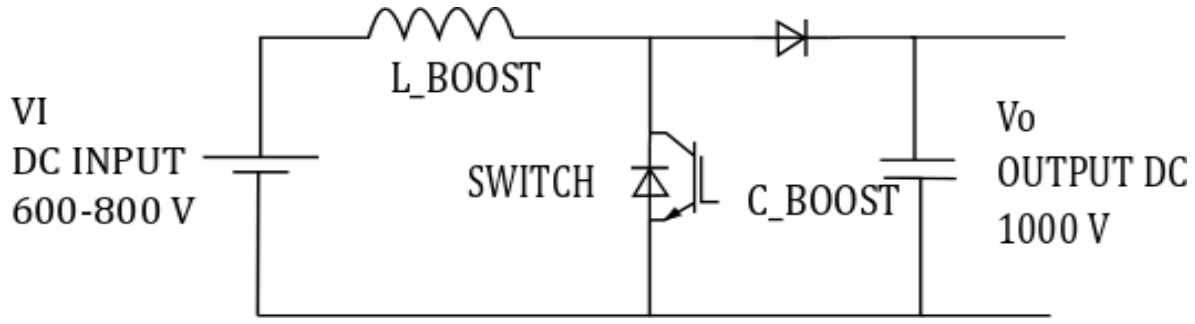

FIG. 31 Boost converter

The output voltage V_0, is a function of the duty cycle D. This is the time in which the switch is on for every cycle. V_I is the input voltage.

$$V_0 = \frac{V_I}{1 - D} \tag{5.2.1}$$

So in order to obtain a controlled output voltage the switch on and off states need to be controlled. This is done in order to obtain a constant output voltage when the input voltage is variable. Then a closed control loop can be implemented. The actual controller is designed in section 5.3.1.

The output voltage is measured and compared with the reference. This error is then feed into a PI controller in order to make it faster and have no error in steady state [31]

This kind of converter is usually used for low power applications. In order to use it for high power a number of them can be connected in series or in parallel, as in [32] The efficiency of these systems is quite high, as much as 98% [18] .

This converter is simple and efficient, there is no need for a transformer. But no big gains can be achieved. Moreover, in high voltage and high power systems its reliability and performance need to be further tested.

Resonant converter

A resonant converter is based on the resonance of inductors and capacitors in order to creating a step-up voltage. A square wave is applied to the L-C section in between, also called resonant tank, as in FIG. 32. This resonant system has a resonance frequency f_0,calculated as in (5.2.2). By changing the frequency of the square wave the magnitudes of the current and voltage out of the resonant part can be controlled. This voltage is then rectified using a diode rectifier.

$$f_0 = \frac{1}{2\pi\sqrt{L_R C_R}} \tag{5.2.3}$$

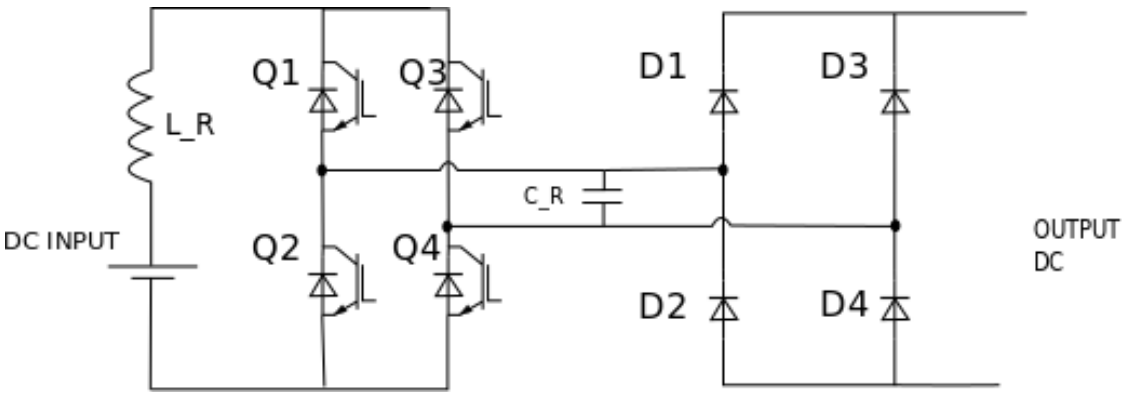

FIG. 32 Resonant converter

The advantage of this option is that high gains can be achieved without using a transformer. The efficiency is not very high, about 90%, and the high step-up is limited to frequency band around the resonant frequency and is not very wide [30] **Fehler! Verweisquelle konnte nicht gefunden werden.**.

5.2.2 Insulated converter

In this type of converters, there is a galvanic insulation between the two different DC voltages. There is a high frequency transformer in between, that creates the insulation. The switches at the low voltage side create a high frequency voltage that is fed into the transformer. This changes the voltage to a higher level, which is then rectified. A typical converter topology is shown in FIG. 33.

This way very high step-up between the input and the output voltages can be achieved. The insulation between voltage levels makes it possible to use lower rated switches in the LV side.

The main issue is the design of the transformer. The high frequency of the system makes the design complex in order to avoid losses, such as dielectric losses in insulation and core losses. High efficiency has been achieved in prototypes for low power, up to 98% [30]

There are many different topologies for this kind of converters but in this case, a simple one is used.

Full bridge converter

In this configuration, a high frequency voltage is fed to a HF transformer that steps it up to a higher voltage level. The input voltage is created using four switches. The voltage created is a square wave. The harmonics this wave carries are significant, but since the transformer is a large inductance, the output wave is smoothed. Anyway, the output voltage is again rectified, so its shape is not that important.

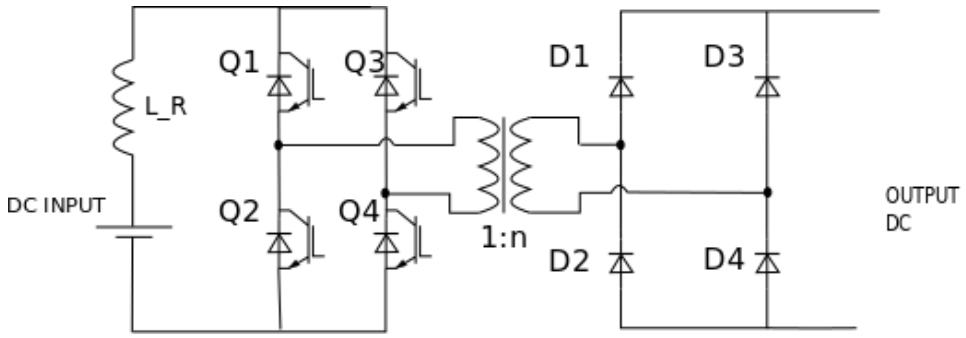

FIG. 33 Full bridge converter, with only one active side on the left

In a real design, this square high frequency signal would create big losses in the iron of the transformer. It is also significant in the HV part of the transformer, the losses through the insulation. The transformer design is a complex matter that is out of the topic of this thesis.

5.3 Converter topologies for simulation

In this section, the WECS topologies discussed in chapter 2 are further explained. The final considerations are made for the simulation in Matlab Simulink. Two different topologies are considered as previously explained. First, the conventional PMSG generator with a full-scale converter, for an AC wind farm. Second, the same machine but considering an implementation in a DC wind farm, with DC/DC converters.

The main difference between the options is the converters used. Now the practical considerations are made. The elements of the converters are chosen, in order to obtain their parameters.

5.3.1 WT model for AC wind farm

As said in chapter 3 the turbine is based in the conventional design. A PMSG is connected directly to the turbine hub, without a gearbox. This generator is connected to a full-scale converter. This converter has an uncontrolled diode rectifier, a boost converter and a VSC connected afterwards, the detailed scheme is in FIG. 34.

The generator produces a variable voltage in module and in frequency, the DC/DC boost converter controls the current in order to control the torque of the machine. The VSC then creates an AC with a constant voltage of 690 and 50 Hz. It is also able to maintain a constant voltage of 100 V in the DC side. Finally, a step-up transformer is connected to get 33 kV.

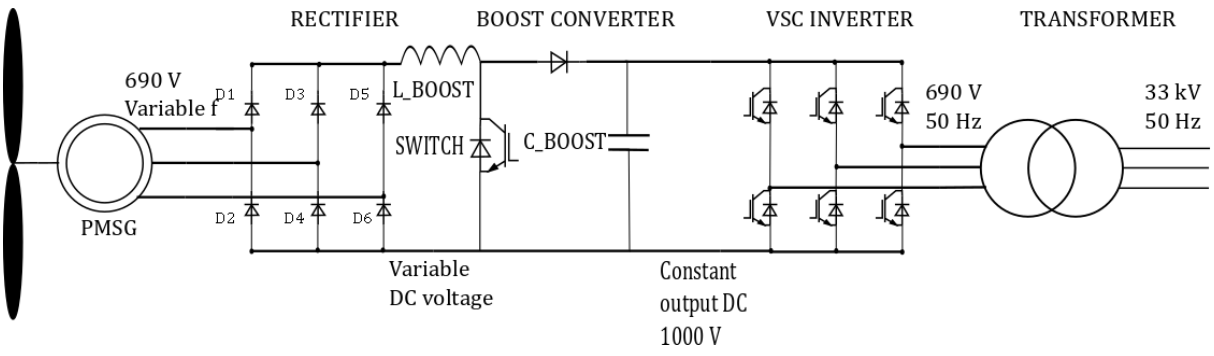

FIG. 34 Detailed scheme of the conventional type IV turbine for the AC wind farm.

The model for the simulation of this thesis is based on a model from the Matlab Simulink libraries [33] In this model, a WRSG is connected to a gearbox, and has a power rating of just two MW. Therefore, changes must be made to create the new model.

In order to obtain a model for the turbine the parameters obtained in section 3.1 are introduced in this model. The WRSG is replaced by the PMSG that was designed in section 3.2. The gearbox is removed and the voltage levels are adjusted.

The control scheme is already tuned. As explained in section 5.1, the VSC inverter control is based on the vector control of the voltage, and is used to control the active and reactive powers out of the system. The control of the boost converter is used to adjust the speed of the machine in parallel with the pitch control.

For this work, the most interesting characteristic of the different converters is their efficiency. In order to calculate it in the simulation, real elements from the manufacturers' portfolio [41] are chosen. The parameters of these elements are then introduced in the model.

In the Simulink software, the converter topologies are introduced using the block called universal bridge. This block implements the same model of IGBT or diode needed in a converter. The same IGBT and diode are used for the AC and DC system converters. They are modeled as real elements, with the losses calculated implementing the resistances and forward voltages in the model.

The details of the diode and IGBT models are included in FIG. 35 and FIG. 36. The conduction losses on the switches are simulated using the resistance values and the voltage drops are introduced as an opposite voltage source. As seen in the pictures, it is also possible to simulate an inductance for the on state, but is not important in our case.

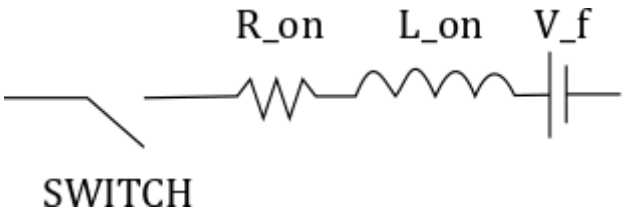

FIG. 35 Simulink model of the diode

In the case of the IGBT switches the switch off losses are also important. These losses are approximated using this approach; when the gate signal falls to zero the current is not immediately cut, but there are the fall time and the tail time where the switch is still conducting, [43]

The parameters and details of the selected elements are depicted in Table 6.

Table 6 Characteristics of the electronic switches.

Element	Parameter	Unit	Value
RECTIFIER and BOOST DIODE	*Resistance of the on state* R_{on}	$m\Omega$	*0.09*
	Forward voltage V_{on}	V	0.790

IGBT, for the VSC and DC/DC converters	*Resistance of the on state* R_{on}	Ω	*0.005*
	Forward Voltage V_{on}	V	0.790

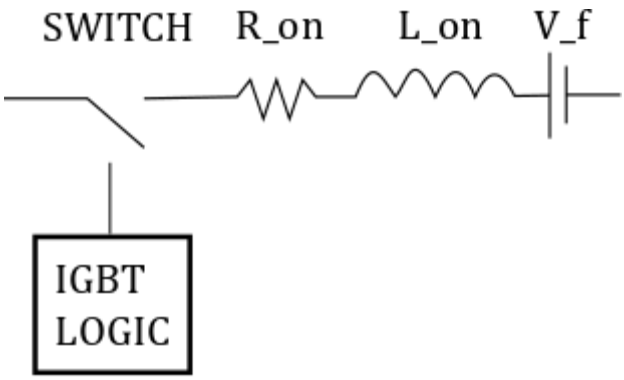

FIG. 36 Simulink model of the IGBT

The last element of the system is the transformer, which is used to step up the voltage to transfer it to the collection grid. The transformer has a high efficiency, that is set by a directive from the European Union [35] . According to this, the efficiency for an eight MVA transformer needs to be at least 99.535%.

The Simulink model of a transformer is quite simple, as in FIG. 37. The model takes into account the winding resistances (*R_1, R_2*) and the leakage inductances (*L_1, L_2*), as well as the magnetizing characteristics of the core, which is modeled by a linear (*R_m, L_m*) branch.

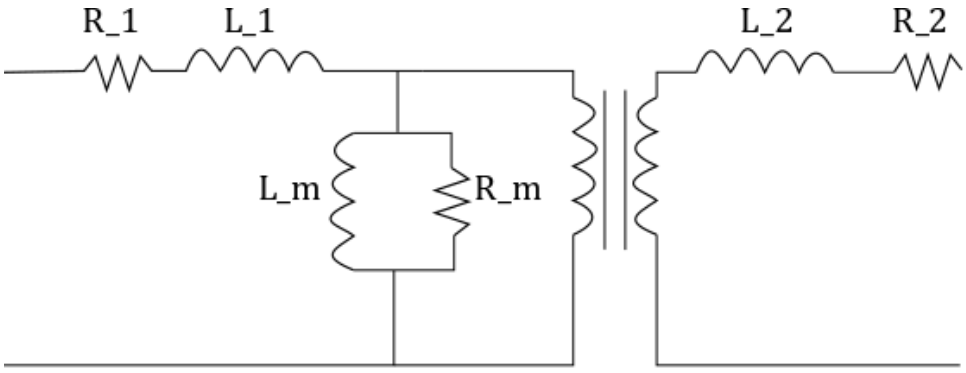

FIG. 37 Two windings transformer model

From [17] the values for the inner resistance and inductance are taken, as in Table 7 Parameters of the step-up transformer. This p.u. values are then used to characterize the parameters of above. More details can be seen in [45]

Table 7 Parameters of the step-up transformer.

Parameter	Unit	Value
Resistance *R*	p.u.	*0.007*
Reactance *X*	p.u.	0.1

5.3.1 WT model for AC/DC wind farm

For the second option, a wind turbine for DC wind farm is modeled. The generator is the same as in 5.3.1. However, the converters are different, since the collection grid works in DC. Therefore, there is no need for an inverter. The boost converter is maintained, in order to control the voltage output. However, in order to step-up the voltage for the collection grid a full-bridge converter is chosen, instead of the inverter and transformer. The scheme is illustrated in FIG. 38.

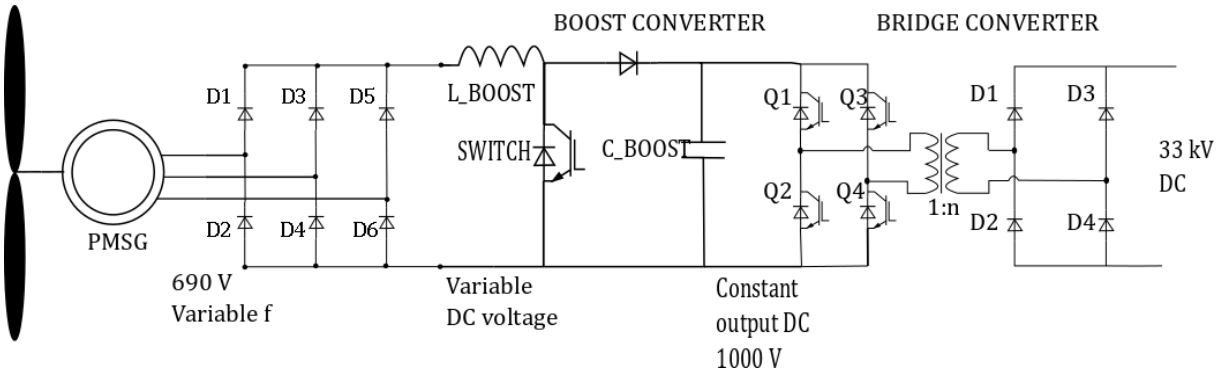

FIG. 38 Detailed scheme of the wind turbine for the DC wind farm.

The voltage is rectified as in the previous model but now the boost converter is used to maintain a constant DC voltage value. It is a simple control solution. The speed control is done just with the pitch control in this model. The Boost converter maintains a constant 1000 V. Then, the bridge converter steps up the voltage to 33 kV for the collection grid.

Nevertheless, the control for the Boost converter is simpler this time. It is only used to have a constant output of 1000 V. In order to achieve that a closed control loop is implemented. This control loop is shown in FIG. 39. The DC voltage out of the boost is measured and the duty cycle of the switch adjusted in order to have always 1000 V, as explained in section 5.2.1. The input voltage is variable, due to the variable speed of the generator.

A Proportionate Integer controller (PI) is used in order to make the control faster and with zero error in the reference. The controller is tuned using the Ziegler-Nichols strategy. This way the errors due to variations in the interference, the input voltage in this system, are minimized [31] .

The full bridge converter is implemented in open loop. The input voltage is constant thanks to the boost converter and the output voltage is therefore constant at 33 kV. The design of the transformer is a crucial point in real systems, but in this case, the model is maintained simple. The system works at 1kHz, in order to make the transformer smaller but the losses in the iron not very large [23] .

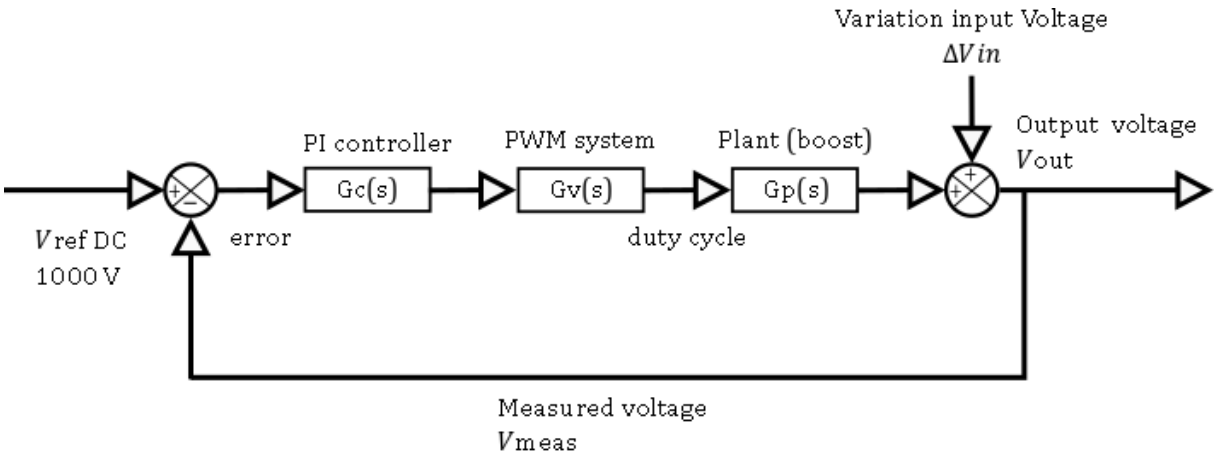

FIG. 39 Detail of the control loop for the boost converter in the AC/DC turbine

The characteristics of the electronic elements are chosen as in the previous model, from Table 6. The transformer as well, as in Table 7.

6 Simulation and results

In this chapter, the simulation of two different wind farms is made in the Matlab Simulink program. The two different wind farms are designed according to the previous chapters.

First, the configuration and topology of the wind farms is depicted. The simulation is explained next and finally the results are shown.

The simulations are made in order to compare the performance of both AC and DC systems. The efficiency of one turbine system is calculated first, to figure out the efficiency of the different elements that compose it. These elements are the generator, rectifier boost converter, inverter and transformer in the case of the turbine for the AC system; and the generator, rectifier, boost and full bridge converter in the case of the turbine for the DC system.

Next, the efficiency of one wind farm branch is calculated. It consists of five turbines connected by submarine cables The losses of the cables are also included in the model.

6.1 AC wind farm model

The first model is based on the conventional variable speed WECS, which is explained in 5.3.1. Then, five of these turbines are connected using a radial connection as in 4.1.1. The first turbine is connected to the second one, this one to the third turbine and so on. Therefore, the current on the last section of the cable is the sum of the current of all the sections. The connection is shown in FIG. 40.

The distance between the machines is usually set to be between five to nine rotor diameters in the dominating wind direction, to minimize wake losses [17] . As was calculated in 3.1 the turbines have a diameter of 144 m. The distance between turbines, and therefore the length of the connection cables, is then selected to be 1 km.

The cable parameters are selected to withstand the whole power of the branch. Therefore, only one cable model is selected according to the maximum power of the branch. The installation of different cables would be more complicated. The five turbines create 40 MW at 33kV. This voltage is the RMS value of the phase to phase voltage. This means that the cable is selected with this voltage rating and for a maximum current of 700 A. This cable is able to carry the current of all the turbines at the rated power.

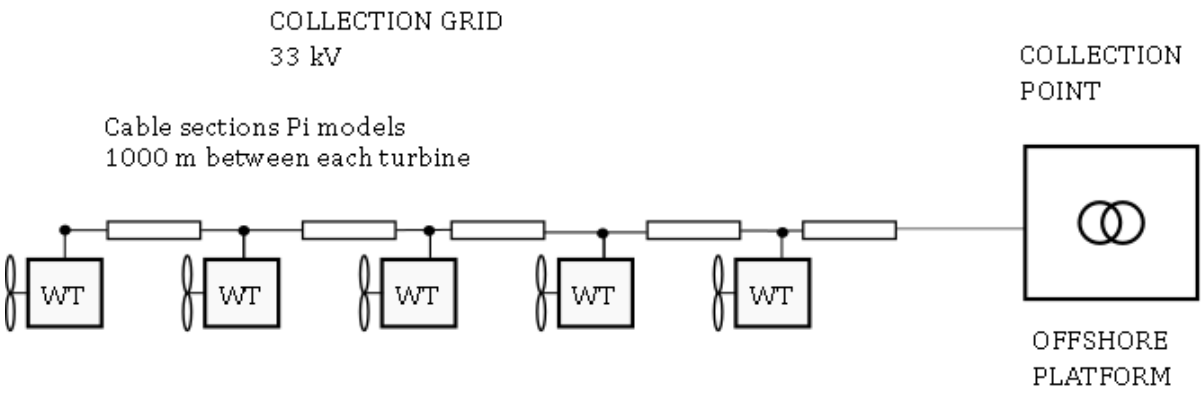

FIG. 40 Branch of the AC wind farm.

This cable is selected from [42] and has the characteristics shown in Table 8. The model for cable simulation is explained in section 4.4.

Table 8 Parameters of the submarine cable.

Parameter	Unit	Value
Inductance per phase per unit of length	mH/km	*0.336*
Resistance per phase per unit of length	Ω/km	0.0625
Capacitance per phase per unit of length	$\mu F/km$	*0.276*
Number of conductors	-	3
Section of each conductor	mm^2	400

6.2 DC wind farm model

This second model is based on the connection of five turbines as in the previous one, but this time the connection is made through DC collection grid. The turbines from section 5.3.1 are used. The connection is depicted in FIG. 41.

In order to make the comparison between the two systems the voltage levels and the cables are the same. However, the cable resistance is different when working at DC. This technology does not suffer the skin effect and does not need reactive power. The same cable with three phases would be installed in the DC wind farm, but since DC needs just two cables the third cable is left unused. Therefore, in the Simulink model of the cable for the DC wind farm is the same as for the AC but just with two phases. As it is shown in section 0 this decision makes the cable conduct too much current.

In this case, the resistance parameter is presented in Table 9. The rest of the parameters are included with the same value, since they are physical properties of the cable.

Table 9 Parameters of the DC submarine cable.

Parameter	Unit	Value
Inductance per phase per unit of length	mH/km	*0.336*
DC resistance per phase per unit of length	Ω/km	0.047
Capacitance per phase per unit of length	$\mu F/km$	*0.276*
Number of conductors	-	3
Section of each conductor	mm^2	400

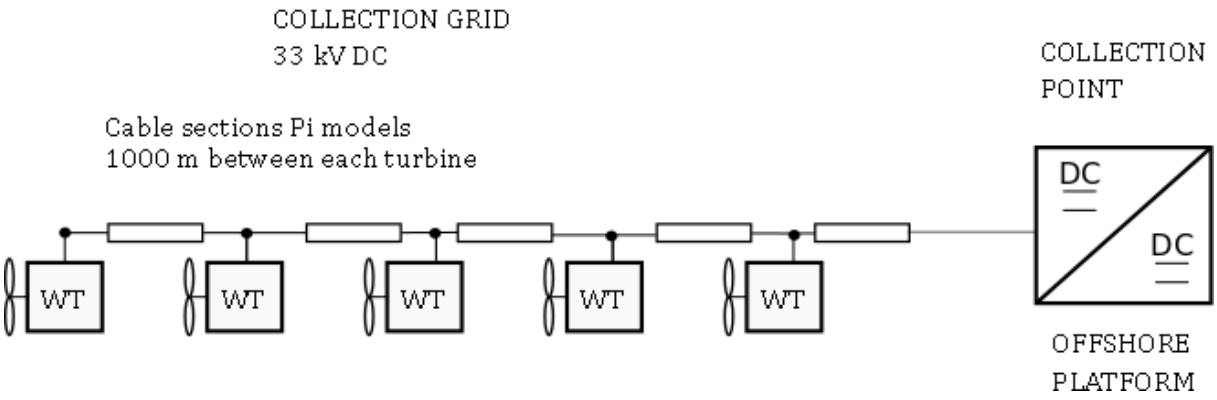

FIG. 41 Branch of the DC wind farm.

6.3 Efficiency calculations

In this section, the considerations for the simulation are made. In order to compare the efficiency and performance of both systems a detailed simulation is made. The different elements are introduced in the software with the data from previous sections. This way, the performance of the system can be addressed accurately.

In order to compare the systems, the efficiency is calculated. In this case, the input mechanical power on the turbine P_m is divided by the electrical power P_{elec} measured out of the element in which the efficiency is calculated:

$$\varepsilon = \frac{P_{elec}}{P_m} \tag{6.3.1}$$

The input mechanical power P_m is the power extracted from the wind that goes into the generator, in the form of rotation. It is calculated by multiplying the mechanical torque T_m with the rotational speed of the turbine ω_{turb}. Since there is no gearbox, the speed of the rotor and the speed of the shaft are the same.

$$P_m = T_m . \omega_{turb} \tag{6.3.2}$$

This mechanical power does not take into account the efficiency of the blades. Therefore, it is the maximum extracted power for each wind speed. This value is then compared with the electrical power out of the whole branch P_{elec}. This value is calculated in different ways for AC or DC systems.

In the AC it is calculated as the active power out of the system. The reactive power is also considered later, but in order to calculate the efficiency only the active portion is used. The phasor equation is used to calculate it, as the Simulink system does it:

$$P_{elecAC} + jQ = V * \bar{I} \tag{6.3.3}$$

Where P_{elecAC} is the active power, Q is the reactive power, V is the voltage and $\bar{I}$ is the complex conjugate of the current. The software uses matrix evaluation to calculate the three phases values.

For DC power systems, the calculation is simpler. The electric power out of the system is calculated multiplying the output voltage V_{DC} by the output current I_{DC}.

$$P_{elecDC} = V_{DC} I_{DC} \tag{6.3.4}$$

6.4 Results

In this section, the two models from sections 6.1 and 6.2 are simulated in the Matlab Simulink software. With the aim of calculating the performance of the systems, a variable wind speed is fed into both systems. This goes through all the range of wind speeds, from the starting wind speed of 5 m/s to the cut-off wind speed of 24 m/s.

The efficiency is calculated as in section 6.3. First, the efficiency of just one turbine system is calculated, for both options. This includes only the generator and converters This way the detailed losses of each element of the system can be quantified. This is done all over the range of wind speed. This way the less efficient element can be identified, for each option.

Next, the simulation of the whole system is done. There are different results from the wind farm branch. First, the efficiency of the system is determined. Additionally, the power output of each of the five turbines is shown for every wind speed.

6.4.1 Wind turbine system efficiency

For this first simulation, the turbine systems for the AC and DC collection grids are simulated at different wind speeds. In each of the simulations, the wind speed is maintained constant until the system works at a steady state. In this state, the power outputs at the different elements of the machine are calculated. This way, the efficiency of the different elements is determined. This method also allows quantifying the output power of the machine at different wind speeds.

In the next graphs, an example of the calculation process is presented, in FIG. 42 and FIG. 43. In them a step in the wind speed is depicted, from 12 m/s to 15 m/s, the step is made with a ramp. Next, the calculated output active power of the AC turbine is presented. In the graph there is an overshoot of the power, caused by the accelerating machine and the control system that is not able to keep up.

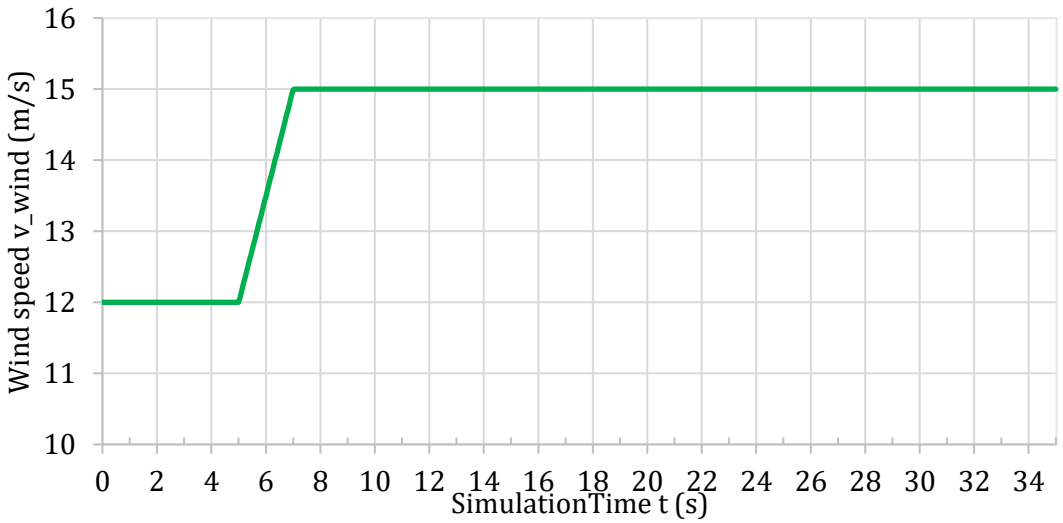

FIG. 42 Wind speed variation

Since the goal of the simulation is to obtain the steady state value of the power output, it is run until this state is achieved. Therefore, the value of the power out of the turbine at this wind speed is calculated by taking the last 5 seconds of the simulation and calculating its average value. This is done to avoid the ripple.

Using this method, in FIG. 44, the output active power of the turbine for the AC system is depicted, and this is the power out of the transformer. It starts working at a wind speed of 5 m/s and is shut off at 24 m/s. There are clearly two regions on the figure. First, the region of maximum power tracking, where the systems extracts as much power as possible from the wind. The second region is the region of constant maximum power, where the system wastes the excess of power in order to obtain the rated power.

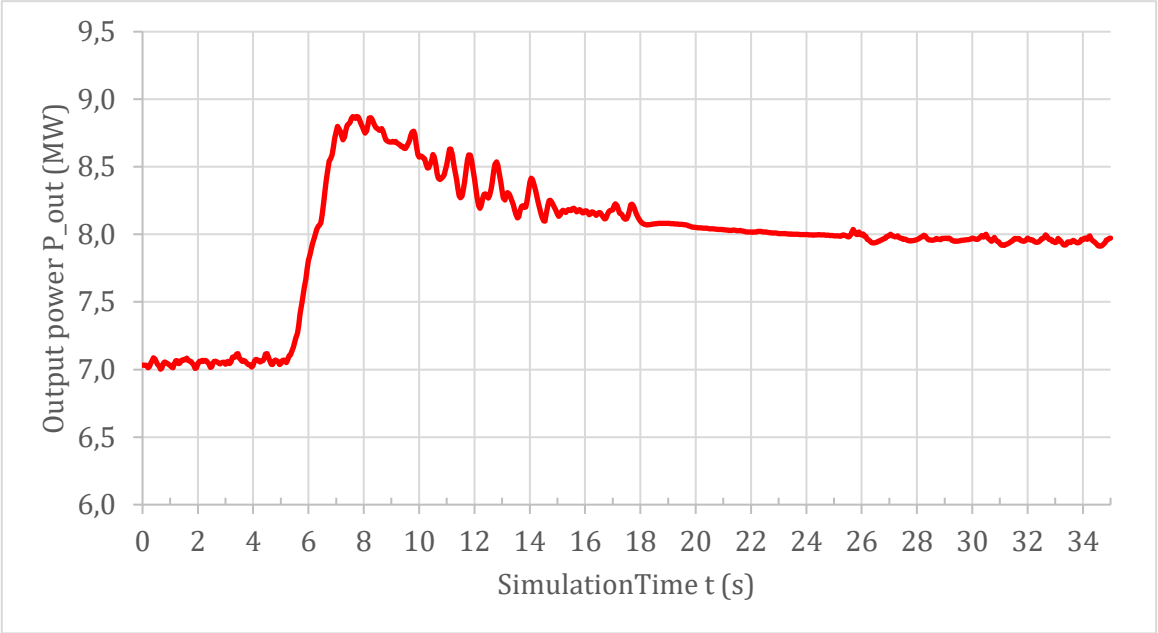

FIG. 43 Output power of one turbine of the AC system with a variable wind speed.

At the rated speed of 12 m /s, the system is supposed to achieve the rated power of eight MW but the losses were not considered at the design phase.

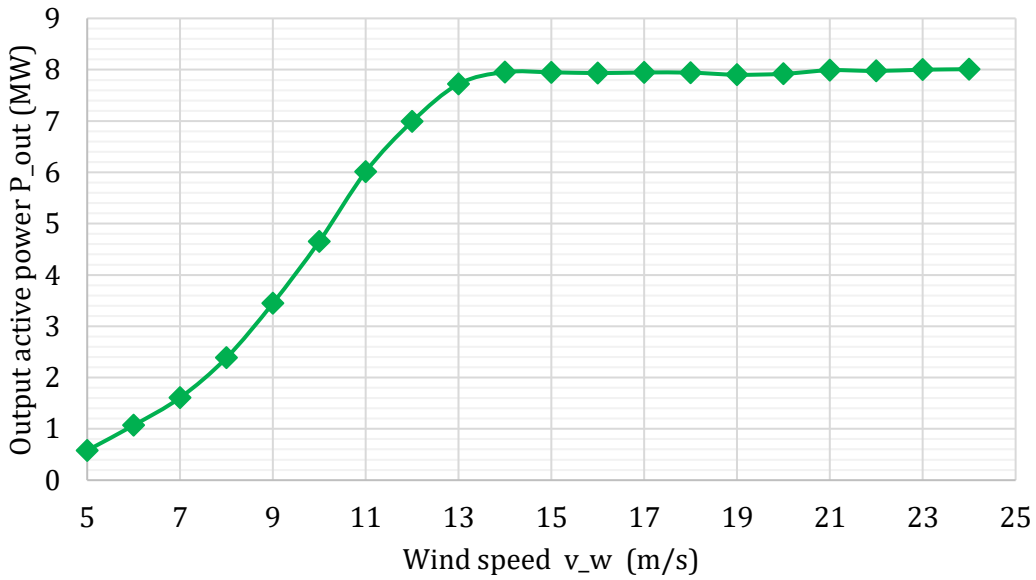

FIG. 44 Power output of the turbine for the AC system for different wind speeds.

In FIG. 45 the efficiency of the system is presented. The efficiency is calculated as explained in section 6.3. From the fact that the efficiency of the system gets lower with the increasing wind speed it can be deduced that the losses increase in the system with higher power. This is due to the increasing current of the system. The efficiency is at its lowest

value at the rated wind speed. From a design point of view, this is not the optimal design. In reality an optimal design is needed. Since this work is focused on the feasibly study, the optimal system is out of our scope.

The average efficiency of the turbine for the whole wind speed range is about 86,84%. This average is calculated only dividing the different values by the number of points calculated. For a more accurate average efficiency, the weight function of the location of the wind farm should be considered, as is done in [43] The efficiency at the rated wind speed is about 85,5%. According to this source, this level of efficiency is reasonable.

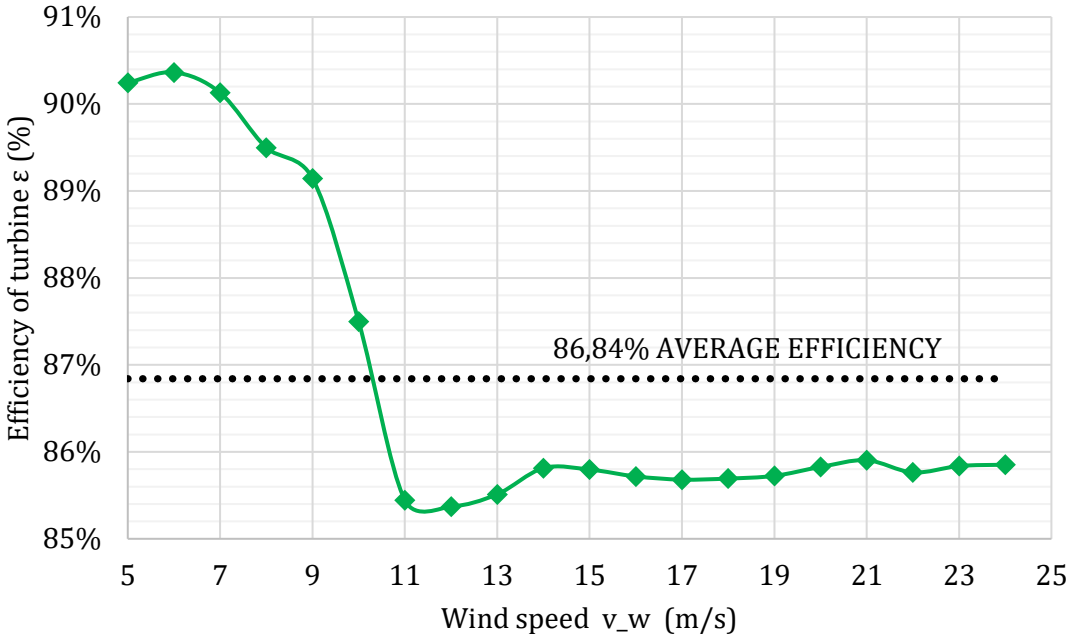

FIG. 45 Efficiency of the turbine for the AC system at different wind speeds.

Next, in FIG. 46, the losses of the different elements of the system are presented. These are, as explained in section 5.3.1, a rectifier connected to the generator, a VSC inverter and a transformer. The power loss is measured in MW.

A great number of facts can be deduced from the diagram. First, the biggest amount of losses occurs in the inverter. These losses increase with the increase in the output power. The losses are produced when the switches of the inverter are used to cut high currents. When the current is high the losses are higher, as explained in section 5.3.1. Therefore, the element that has a major reason for improvements is the inverter.

It is deduced from the graph that the losses in the generator and rectifier are quite big as well. These losses may be lowered by substituting these two systems by a DC generator that does not need a rectifier

To finish with the turbine for the AC system, it can be deduced from the data that, as expected, the transformer does not create a big amount of losses.

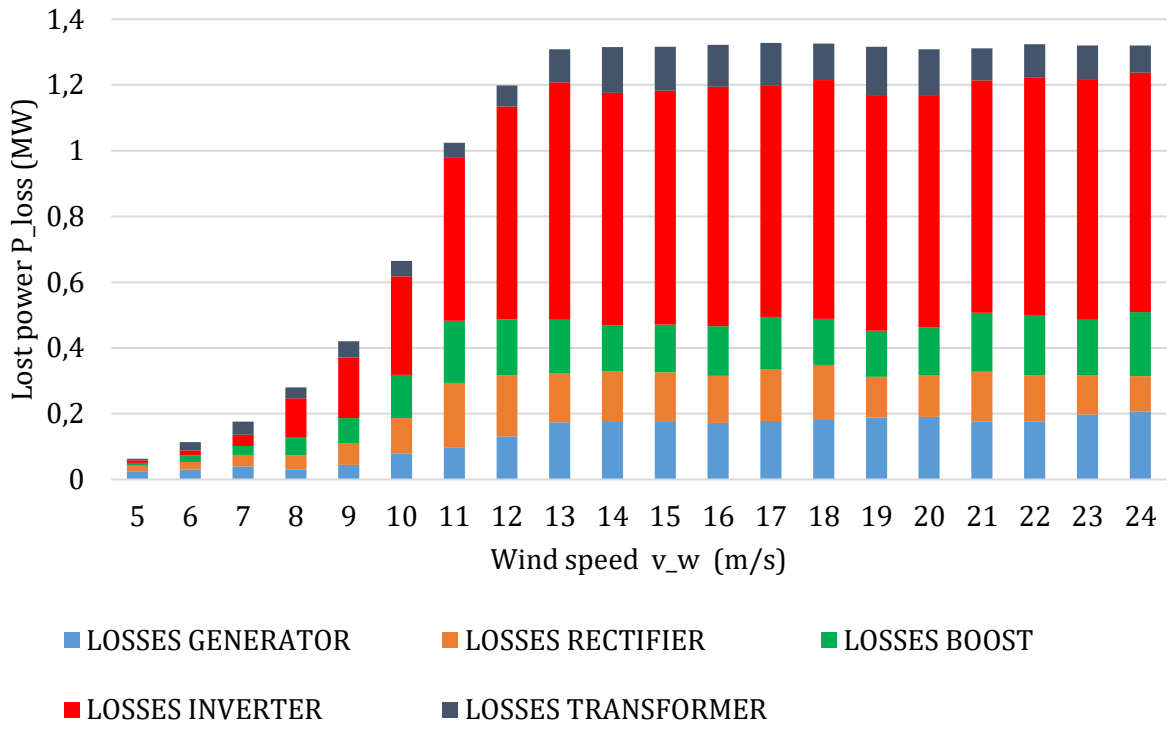

FIG. 46 Breakdown of losses in the AC system.

Now the system for the DC collection grid, the one explained in section 5.3.1 is simulated as well. The turbine is also fed with different wind speeds and the efficiency is calculated.

As a first result, in FIG. 47 the output active power of both turbines can be seen, at different wind speeds. This way, both systems are compared. The turbine for the DC system follows the same working principle with two different work stages, for lower wind speeds and for wind speeds higher than the rated one.

It is clear that the turbine for the AC/DC system extracts at least as much power from the wind as the conventional model described before. As it was explained in section 5.3.1 the selected control system is simple but it is clear that the performance, at least at steady state is as good as in the other system.

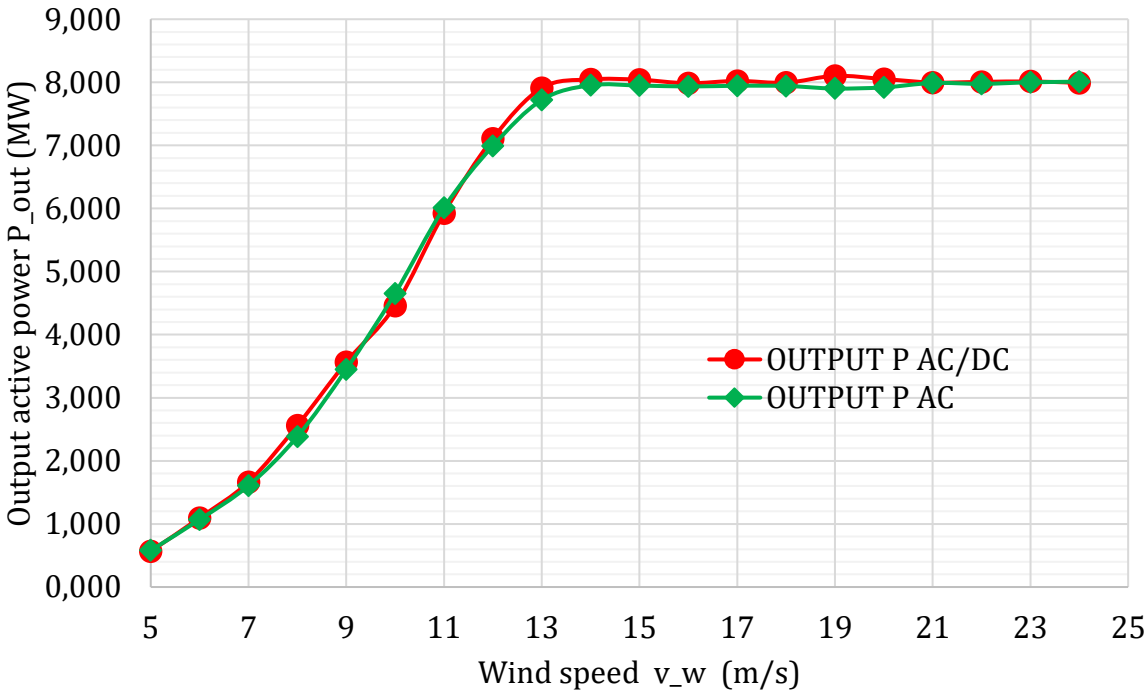

FIG. 47 Power output of the turbines for the AC and DC system for different wind speeds.

Afterwards, the efficiency of the WECS is calculated, as in the previous case. In FIG. 48 the efficiency of both systems is depicted. It is evident, as in the previous case, that the efficiency of the turbine for the DC system changes with the power output of the system. At more power, there is more current and bigger losses.

It can also be seen that although the average efficiency of the AC/DC turbine system is higher, the efficiency of the conventional AC system is higher at the rated power stage. This means that the turbine for the DC system needs more power extracted from the wind in order to generate the eight MW. This involves higher forces in the blades and a higher maximum rotational power.

Finally, the breakdown of the losses in the turbine for the AC/DC system is presented in FIG. 49. As it was clarified in section 5.3.1, the system consists on the generator connected to an uncontrolled rectifier, this one to a boost converter and finally a step-up full bridge converter.

The total losses are higher in this case. The full bridge converter creates almost half of the losses. It is clear then that a more efficient way to step-up the voltage for the collection grid in a DC system is of utmost importance.

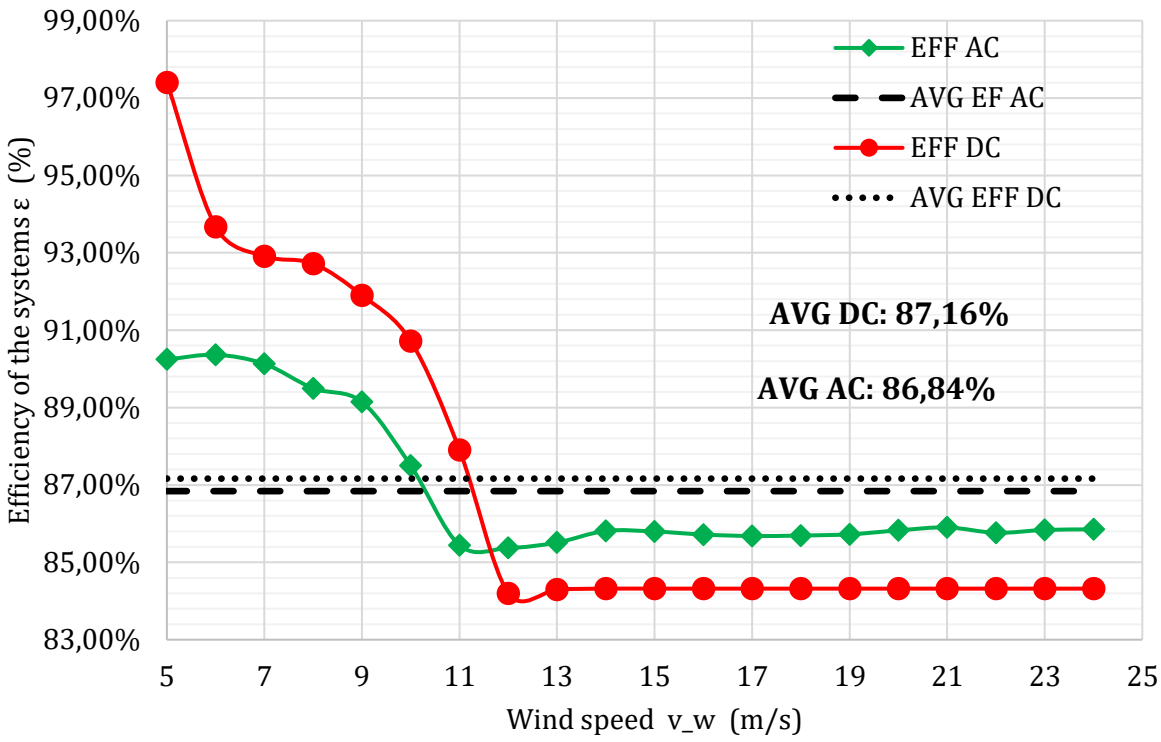

FIG. 48 Efficiency of the turbine for the AC and AC/DC systems at different wind speeds.

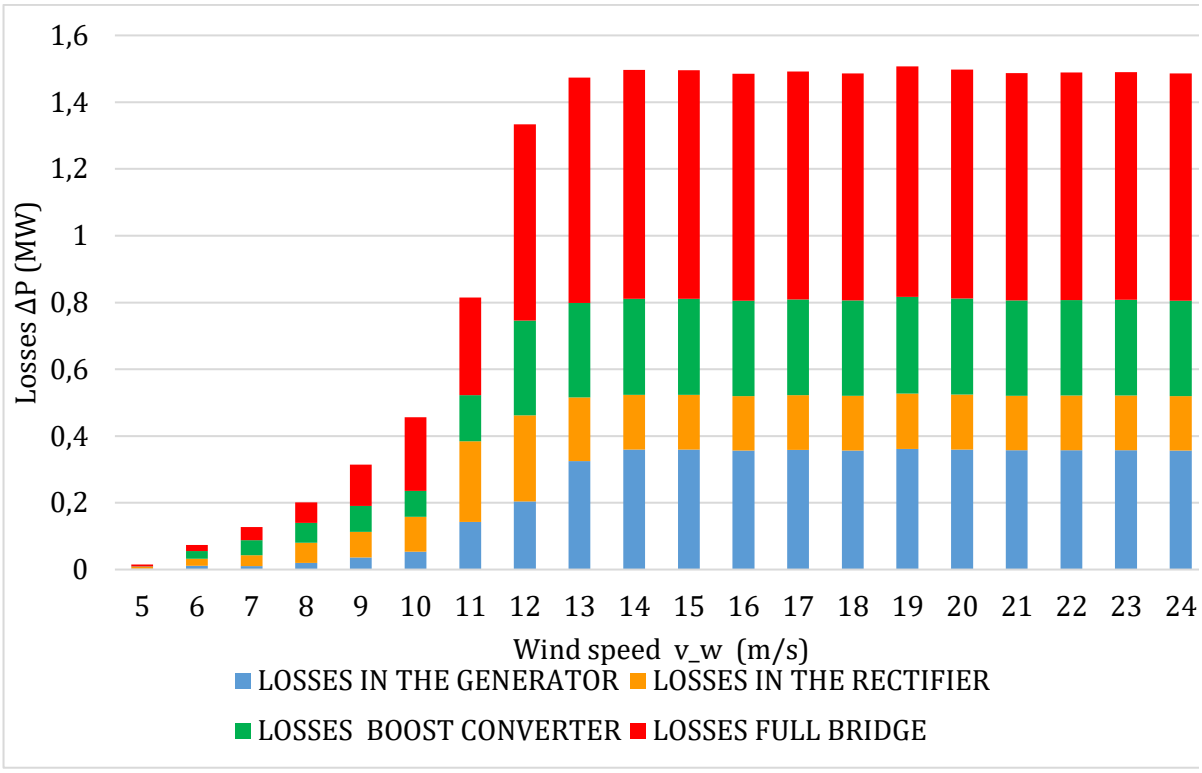

FIG. 49 Breakdown of losses in the turbine for AC/DC system

6.4.2 AC wind farm branch simulation

In this second case, the AC wind farm branch is simulated at different wind speeds. The used system is the one explained in section 6.1, with 5 turbines connected in one branch and connected with submarine cables.

Different results are presented in this section. First, simulations are completed to obtain the output power of the whole system at different wind speeds and the output power of each turbine as well. The losses in the cables are calculated and the efficiency of the whole wind farm as well. Finally, the reactive power needs of the system are calculated.

As a first result, the power output of the system is presented, for the whole wind speed range. In FIG. 50 this power output is shown. Its shape is quite similar to the graph in FIG. 44, where the power output of just one turbine is shown, but this time for five turbines. The most important fact is that the rated power is not achieved at the rated wind speed, due to the losses. This power is only 34.33 MW,

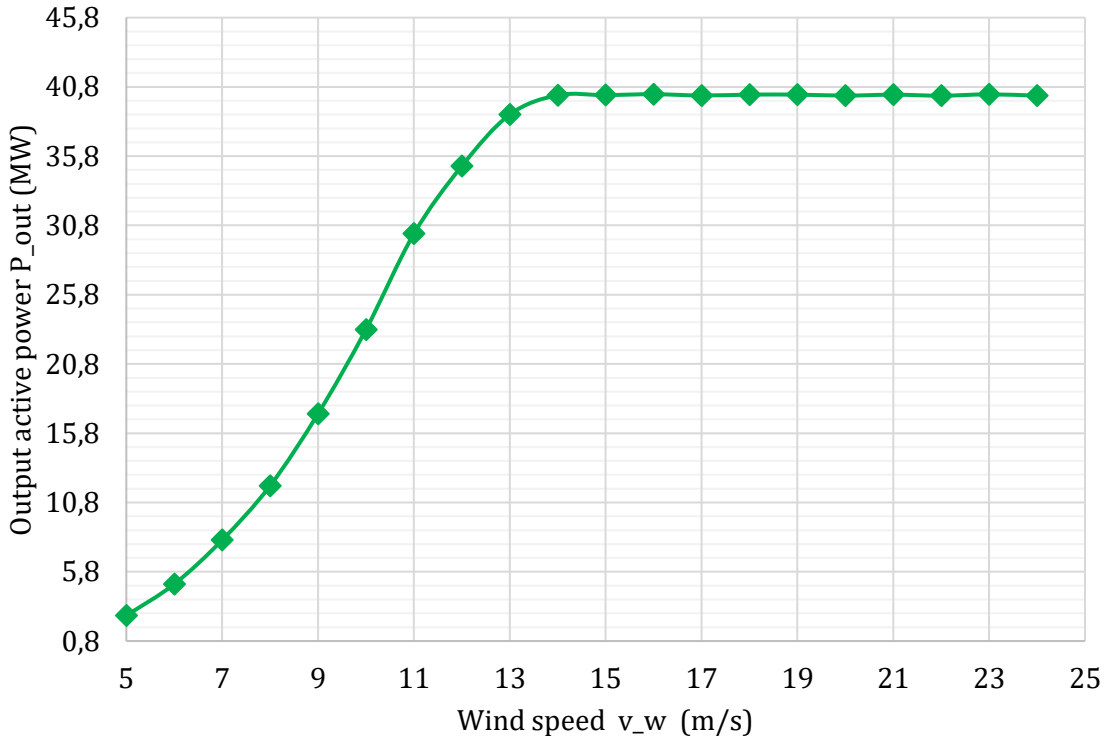

FIG. 50 Active power output of the AC wind farm branch at different wind speeds.

In the next graph; FIG. 51, the efficiency of the system is depicted along with the efficiency of the turbine from the previous section. It is clear that the efficiency is lower in the wind farm branch. In the phase at rated power, it is clearly because of the losses in the cables. However, for the phase at lower wind speed the explanation is not so clear.

As it is shown later in FIG. 53, the needed reactive power of the system is higher at lower wind speeds, when the power is lower. This makes the control system accelerate the machine in order to create more rotational power but the inverter does not generate enough reactive power. As said before, the control system would need an improvement.

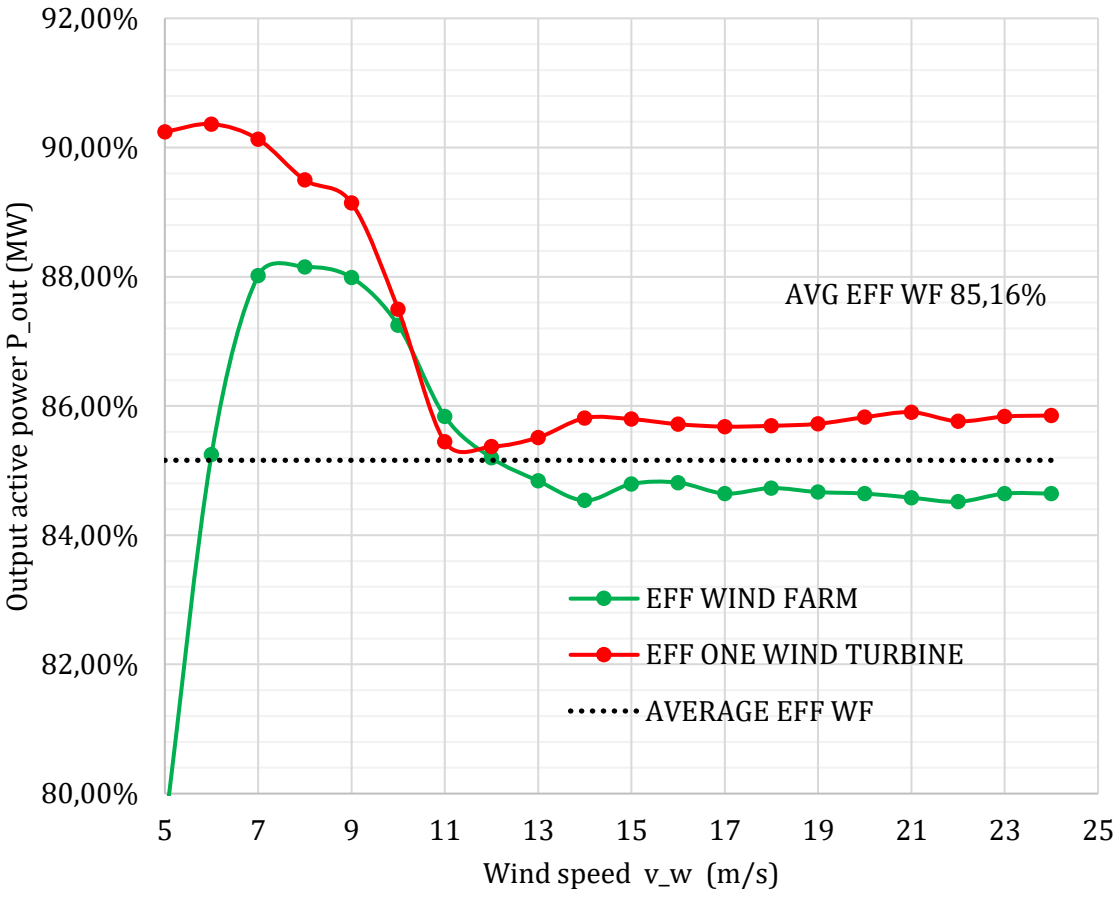

FIG. 51 Efficiency of the AC wind farm branch and the AC wind turbine system

Furthermore, the losses in the cable system are presented in FIG. 52. The current out of the system, in RMS values, is also presented in the graph. As said, the losses in the cables are not significant until the rated wind speed is achieved. The losses are proportional to the current and the current is highest at this point.

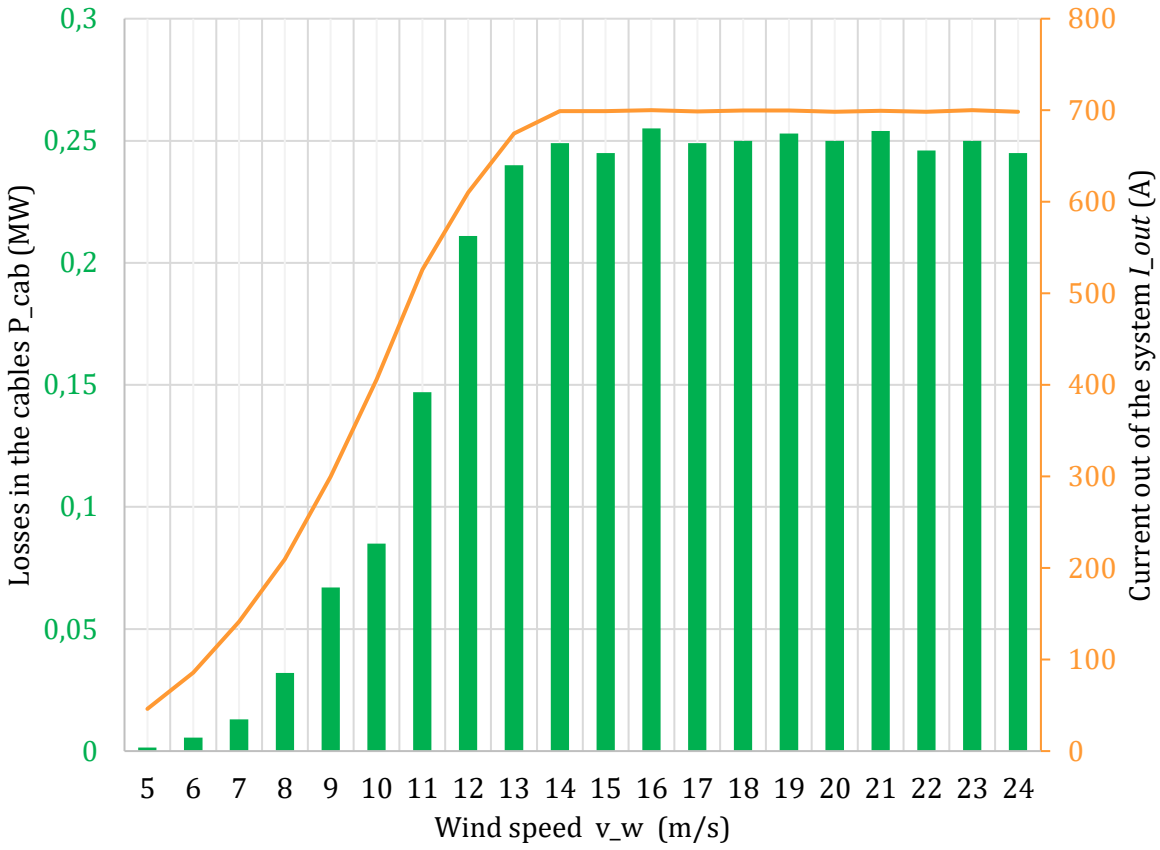

FIG. 52 Cable loses and output current at the AC wind farm

On the next result, the reactive power needed by the system is presented in FIG. 53. As explained before, the system needs more reactive power for the cables at lower rated power. There is the static reactive power that is needed when the cable is energized and the dynamic reactive power that depends on the current through the cables.

When the generators work at lower power, there is no reactive power generation in the inverters and with an increasing amount of current the reactive power is also increasing. When the wind speed arrives at the rated value, the inverter is able to create more reactive power to compensate. At higher current higher reactive power is needed, but in this case the generated one is able to compensate the dynamic value and even cut some of the static reactive power.

This amount of reactive power may seem low in a 40 MW system but the length of the cables would be too short to arrive to the shore. In a real system there would be many more turbines and more cables, plus the connection to shore, which would be the critical point. Therefore, in a real system a reactive power compensation system would be necessary.

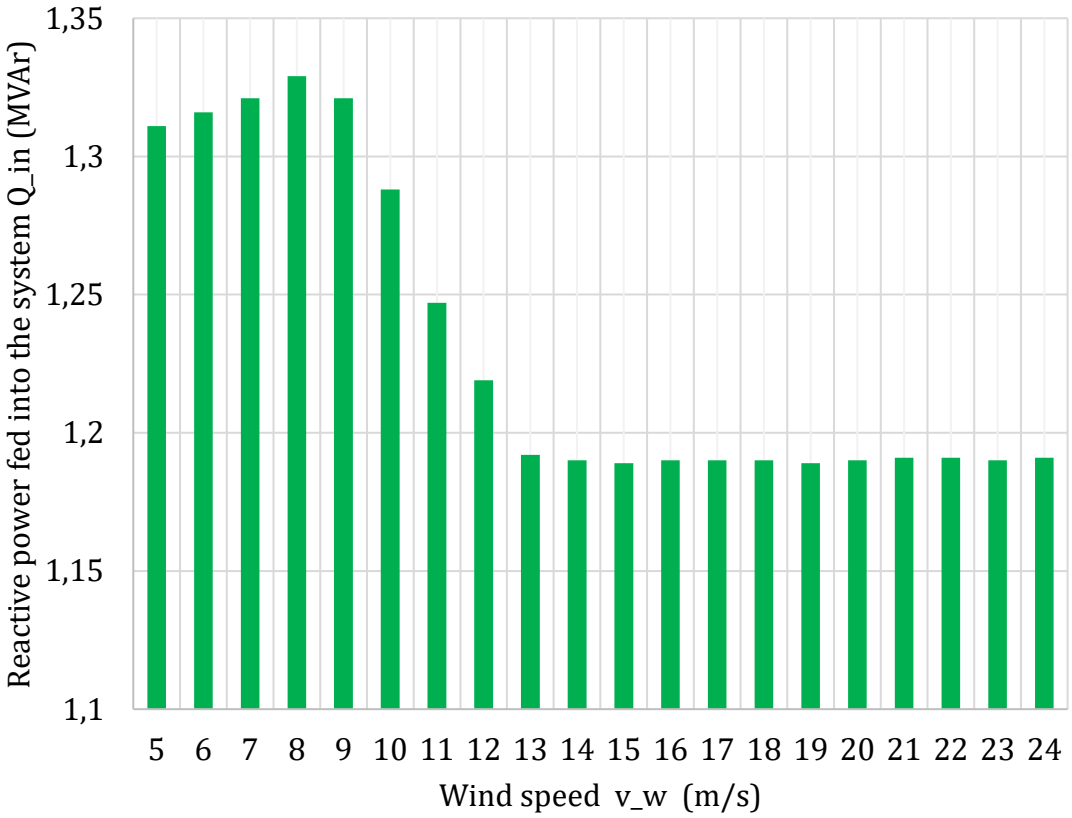

FIG. 53 Reactive power needs of the AC wind farm branch

6.4.3 AC/DC wind farm branch simulation

As with the previous model, in this section the DC wind farm branch presented in section 5.3.1 is simulated over all the wind range. As a result, the output power of the system, the efficiency and the losses in the cables are shown. In addition, the power of the different turbines is shown in this case.

In the graphs, results from both systems are presented, in order to make the comparison easier.

As said, the power output of the DC wind farm branch is presented in FIG. 54, together with the power output of the AC wind farm branch. It is clear that the power output of the DC system is similar to the conventional model It shows that the created system is able to generate the same amount of power as a more conventional system, even with a simple configuration.

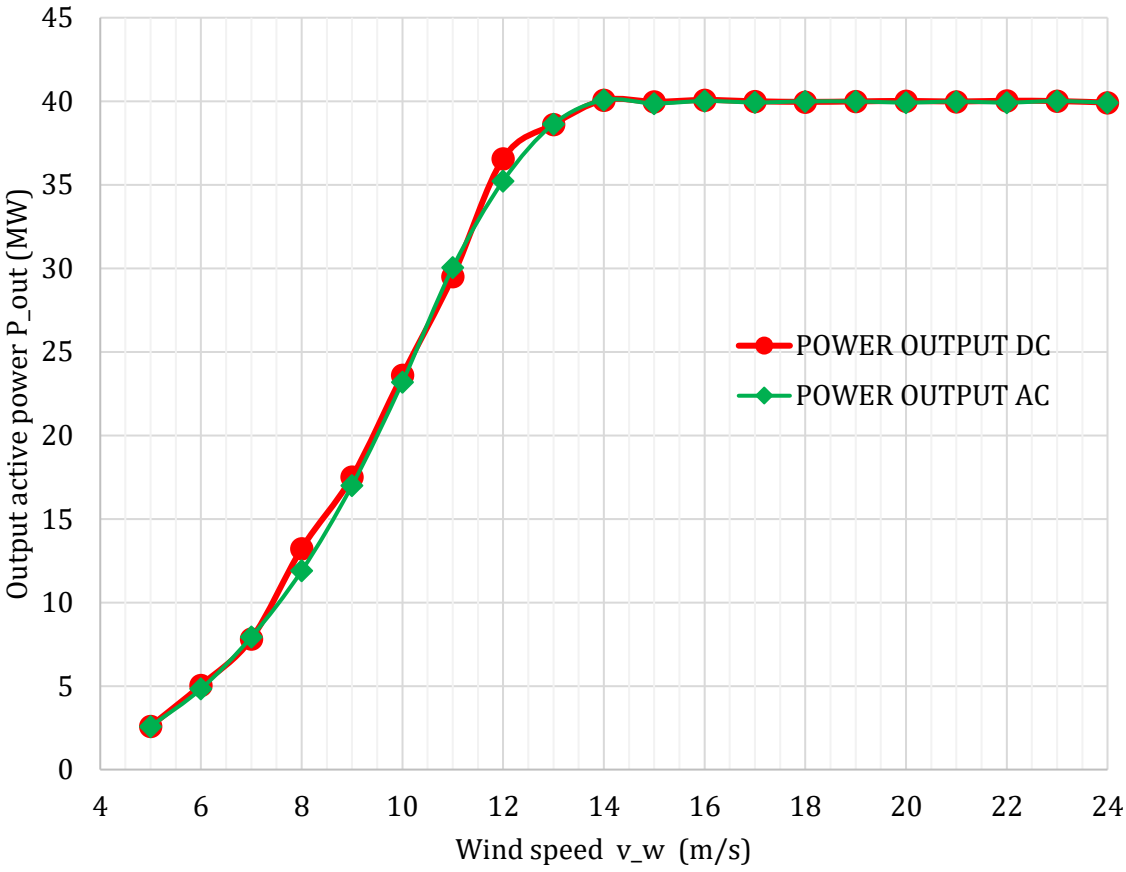

FIG. 54 Active power output of the AC and DC wind farm branches at different wind speeds

In the next graph, in FIG. 55, the efficiency of the AC and DC systems is shown. As with the turbine systems in section 6.4.1, it shows a development similar to the graphs of the turbine systems. The DC wind farm branch has a higher efficiency for lower wind speeds but lower in the rated wind speed stage. In the previous section it was explained how the reactive power makes the AC system so inefficient at low wind speeds.

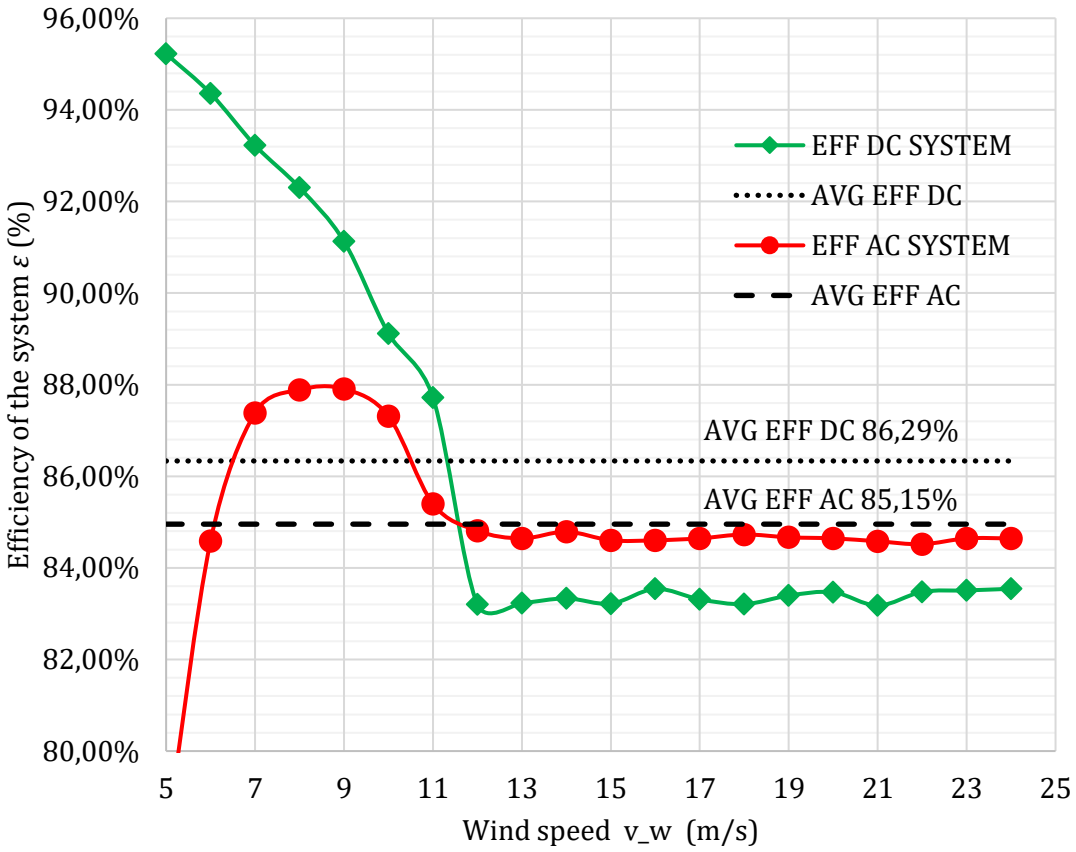

FIG. 55 Efficiency of the AC and DC wind farm branches

Following this development, the cable losses for the DC system in FIG. 56 show a similar trend as in the AC system. As in the previous case the losses are proportional to the current, thus, the quantity increases with the wind speed. The losses are, however, higher, about 60 % higher.

This is due to the fact that the cable was not designed for a DC system. In this case two phases of the cable have to transmit 1,2 kA in the calculated peak current. This makes the losses in the cable higher for the DC system, since the cable is overcharged.

For the same power rating and with the same voltage levels a DC system has higher currents than in an AC system [46] . Anyway, the losses are still just about a 1% of the output power. The efficiency difference is mainly because of the losses in the converters that were depicted in section 6.4.1.

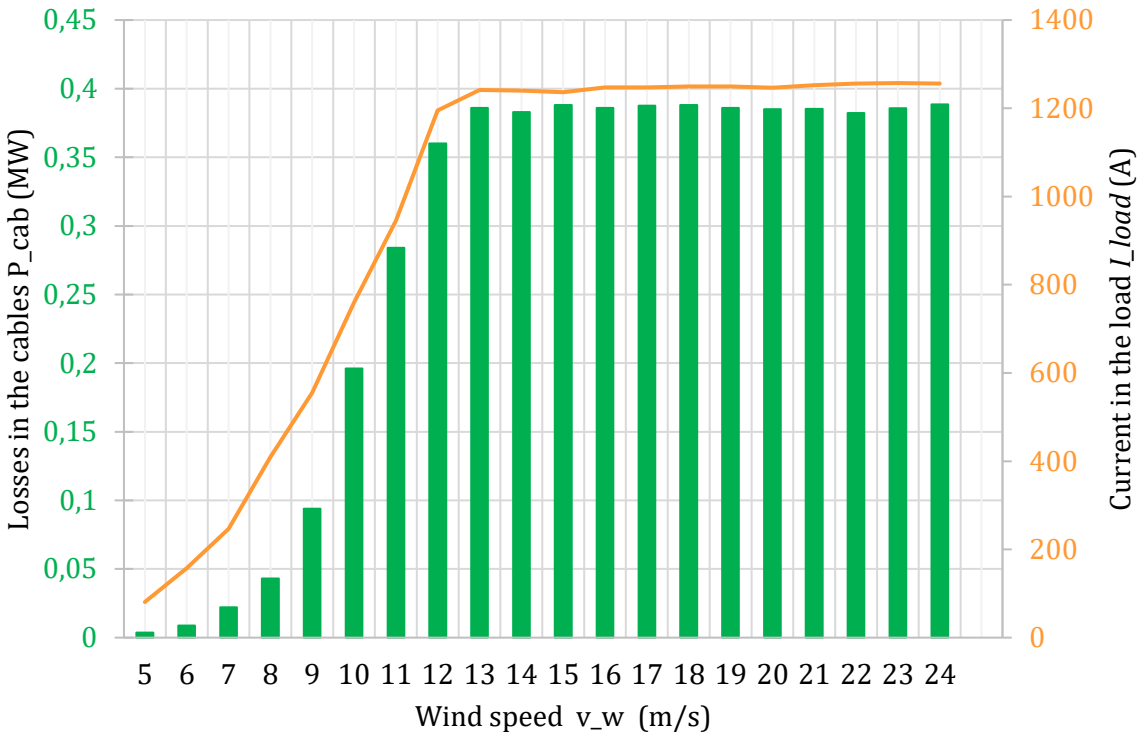

FIG. 56 Cable loses at the DC wind farm branch

Nevertheless, there is an interesting result in FIG. 57. It can be observed that the generated power by each of the turbines is not equal, even if they are receiving the same amount of power from the wind.

At the different wind speeds, the first turbine in the branch, the one that is nearest to the PCC is the one that produces more. This is due to the control system of the turbines. The voltage output of each turbine is the same, but the current out of each of them is not. Even if the same wind speed is fed into all the turbines.

The current is uncontrolled and this affects the torque of the generator. The designed control system is just controlling the output voltage of each turbine. This means that the system is clearly not working at its maximum potential.

Therefore, the control system is too simple and is not able to manage the control of the power in the DC bus. In practice, a more complicated control strategy is needed.

This is not the case in the AC wind farm, in which every turbine is creating same amount of power at every wind speed. However, the system is connected to the grid from which it takes the reference voltage for the inverters and the reactive power it needs.

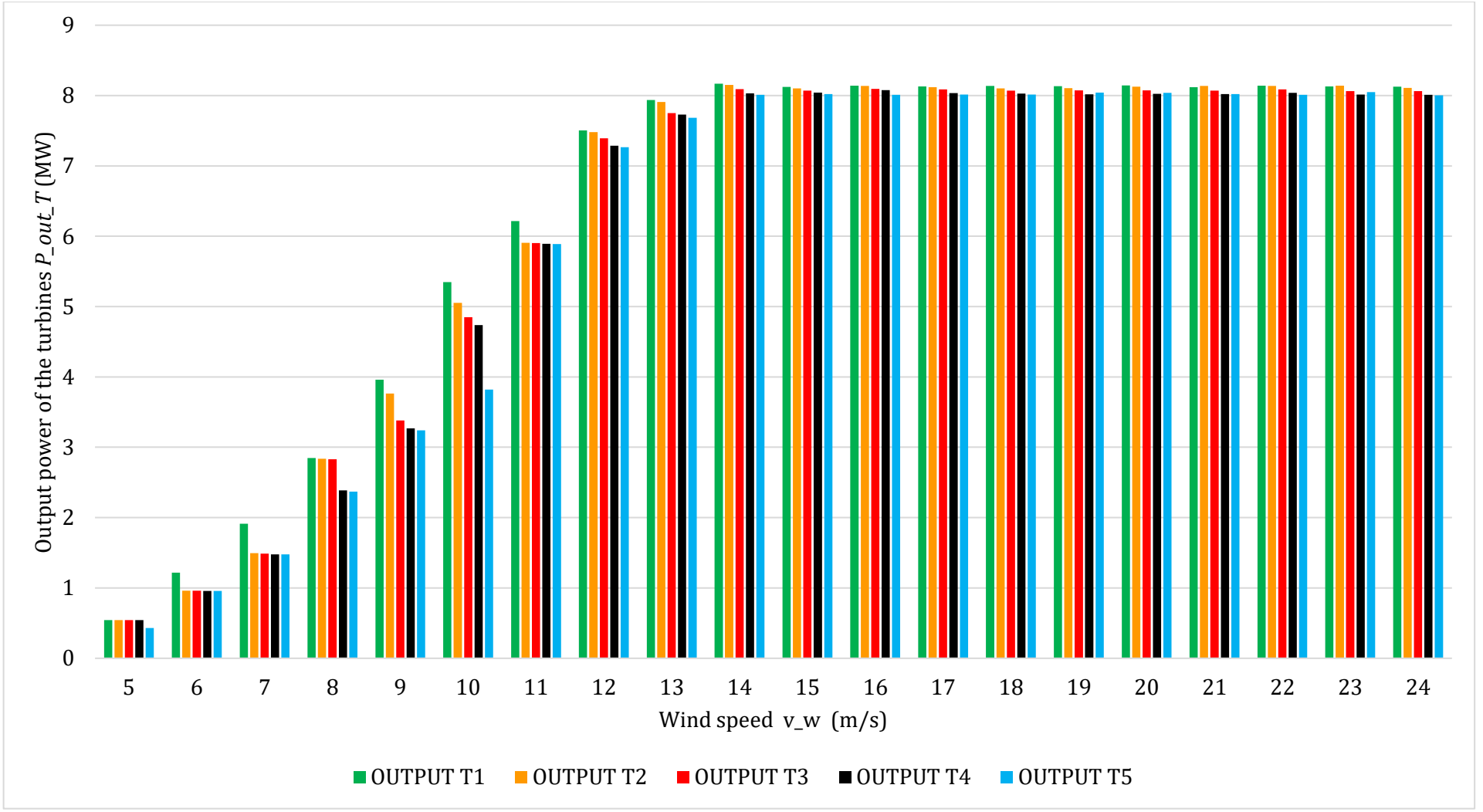

FIG. 57 Output power of each turbine of the DC wind farm branch at different wind speeds

7 Conclusions and future work

In this final section of the work a resume of the project is done and the final conclusions are explained. An introduction to future possible development projects is also done.

It can be deduced from the extensive information that the WECS are a mature technology and offshore wind farms are currently being developed all over the world with different configurations. Taking all this info into account two different systems are created and simulated.

The first fact that needs to be pointed out, is that through this work it is once again proven that DC technology is feasible, and as the results show, at least as efficient as the conventional AC technology. It was possible to create a working model for a DC wind farm and compare it with the conventional AC model.

The created system had adequate efficiency. The main source of losses was the converters, as expected. There is a lot of room for improvement in this. The efficiency of both types of collection grids is pretty similar.

One of the main challenges was to select the different elements that would go into the system. It was important to make it simple, but the results should be accurate as well.

However, due to some unexpected problems with the software, the dynamic performance of the system remains unclear. Thus, the control system would be the part of the work where more improvement can be made. It was always an objective to keep the models as simple as possible, but one of the problems encountered on the process is that it may not be that simple to find an adequate control for DC technology.

Therefore, aside from the improvement of the converters, which is important, an investigation on the dynamics and control capabilities of DC grids should also be implemented. It is a new and complex concept so the challenges are great but the technology has also promising advantages.

There is no need for reactive power compensation in the DC system. The system efficiency has a lot of room for improvement but its results are similar to the results for the AC system and there is no need for bulky transformers, which could be an advantage in offshore systems.

However, DC systems have unproven durability, which is caused by the immaturity of the technology. There is, as well, more need for costly converters and there is still no perfect choice for step-up converter. This problem, compared with the proven and trustworthy transformers is one of the main reasons for the lack of real application.

Nevertheless, the simplicity of the chosen elements is still an advantage and it helped to finish the project. Although there are a lot of concepts that were not taken into account. Concepts such as, protection systems for DC grids, realistic and accurate converters and how would these behave in case of a fault. One of the mains points that did not make it into the scope of this work would be the dynamic performance of the system and it should be further investigated.

8 Literature

[1] Renewable Energy Policy Network for the 21st Century, "Renewables 2017 global status report", Internet: http://www.ren21.net/wp-content/uploads/2017/06/17-8399_GSR_2017_Full_Report_0621_Opt.pdf , June, 2017[Nov. 10, 2018].

[2] T. ACKERMANN et al. *Wind Power in Power Systems*. Wiley, Second Edition 2012.

[3] U. S. Department of Energy, "*Wind Technologies Market Report",* Internet: https://www.energy.gov/sites/prod/files/2017/08/f35/2016_Wind_Technologies_Market_Report_0.pdf . Aug., 2017 [Nov. 24, 2018].

[4] Global Wind Energy Council, "Global Wind Statistics 2016", Internet: https://www.gwec.net/wp-content/uploads/vip/GWEC_PRstats2016_EN_WEB.pdf , June, 2016 [Nov. 17, 2018]

[5] "Aerodyne wecs" , Internet: wind turbine models website, https://www.en.wind-turbine-models.com/turbines/1116-aerodyn-scd-8.0-168#powercurve , March 3, 2015 [Nov., 2018].

[6] U.S. Department Of Energy, "Levelized Cost of Energy Report", Internet: https://www.energy.gov/sites/prod/files/2015/08/f25/LCOE.pdf. Aug., 2015 [Nov., 2018].

[7] Wind Europe, "Annual Offshore Statistics", Internet: https://windeurope.org/wp-content/uploads/files/about-wind/statistics/WindEurope-Annual-Offshore-Statistics-2016-Infographic.pdf. Aug., 2016 [Nov., 2018].

[8] Berkeley Lab Electricity Markets & Policy Group, "Reducing Wind Energy Costs through Increased Turbine Size: Is the Sky the Limit?", Internet: https://emp.lbl.gov/sites/all/files/scaling_turbines.pdf , Nov., 2016 [Nov., 2018]..

[9] Tennet GmbH, "BorWin 2 Project Brochure", Internet: https://www.tennet.eu/de/unser-netz/offshore-projekte-deutschland/borwin2/, June, 2018 [Nov., 2018].

[10] Kira, Croog, "*Harvesting The Wind: The Physics of Wind Turbines"*, Carleton College , Internet: https://apps.carleton.edu/campus/library/digitalcommons/assets/pacp_7.pdf, Apr., 2005 [Nov., 2018].

[11] Siemens AG; "Wind Turbine models catalog", Internet: https://www.siemensgamesa.com/products-and-services/offshore/wind-turbine-sg-10-0-193-dd . Aug., 2018 [Nov., 2018].

[12] Thomas Haugsten Hansen, “Offshore Wind Farm Layouts, Performance Comparison for a 540 MW Offshore Wind Farm”, Master Thesis, Norwegian University of Science and Technology, 2009.

[13] Christoph Steitz; "Vestas bets on geared turbines to propel it to margin goal", Reuters, Internet: https://www.reuters.com/article/us-vestas-wind-results-gearbox/vestas-bets-on-geared-turbines-to-propel-it-to-margin-goal-idUSKBN1FS2X0, Feb. 8, 2018 [Nov., 2018].

[14] H. Polinder, F. F. A. Van Der Pijl, G. -. De Vilder and P. J. Tavner, "Comparison of direct-drive and geared generator concepts for wind turbines", in *IEEE Transactions on Energy Conversion*, vol. 21, no. 3, pp. 725-733, Sept. 2006 [Nov. 2018].

[15] Y. Liu, M. Noe and M. Doppelbauer, "Feasibility Study of a Superconducting DC Direct-Drive Wind Generator," in *IEEE Transactions on Applied Superconductivity*, vol. 26, no. 4, pp. 1-6, June 2016 [Aug. 2018].

[16] J. Wang et al., "Design of a Superconducting Synchronous Generator with LTS Field Windings for 12 MW Offshore Direct-Drive Wind Turbines", in *IEEE Transactions on Industrial Electronics*, vol. 63, no. 3, pp. 1618-1628, March 2016, [Jul., 2018]

[17] Thomas Haugsten Hansen, "Offshore Wind Farm Layouts", Master Thesis, 2009, Norwegian University of Science and Technology, 2009 [Jun., 2018].

[18] Olof Martander, "DC Grids for Wind Farms", Thesis for The Degree of Licentiate of Engineering, Chalmers University of Technology, 2002 [Jun., 2018].

[19] Stefan Lundberg, "Wind Farm Configuration and Energy Efficiency Studies-Series DC versus AC Layouts", Thesis for the degree of doctor of philosophy, Chalmers University of Technology, 2006 [Jun., 2018].

[20] A. Madariaga, J.L. Martín, I. Zamora, I. Martínez De Alegría, S. Ceballos, "Technological Trends in Electric Topologies for Offshore Wind Power Plants", *Renewable and Sustainable Energy Reviews*, Volume 24, 2013 [Jun., 2018]

[21] H. Polinder, D. Bang, R. P. J. O. M. Van Rooij, A. S. Mcdonald and M. A. Mueller, "10 MW Wind Turbine Direct-Drive Generator Design with Pitch or Active Speed Stall Control", *2007 IEEE International Electric Machines & Drives Conference*, Antalya, 2007 [July, 2018].

[22] K. Eriksson et al, "System Approach On Designing an Offshore Wind Power Grid Connection", ABB Library, April 2005, [July, 2018]

[23] C. Meyer, M. Hoing, A. Peterson and R. W. De Doncker, "Control and Design of DC Grids for Offshore Wind Farms," in *IEEE Transactions on Industry Applications*, vol. 43, no. 6, pp. 1475-1482, Nov.-Dec. 2007 [Sep. 2018].

[24] Lena Max, "Design and Control of a DC Collection Grid for a Wind Farm", Thesis for The Degree of Doctor of Philosophy, Chalmers University of Technology. 2009 [Sep. 2018].

[25] J. Yang, J. E. Fletcher and J. O'Reilly, "Multiterminal DC Wind Farm Collection Grid Internal Fault Analysis and Protection Design," in *IEEE Transactions on Power Delivery*, vol. 25, no. 4, pp. 2308-2318, Oct. 2010 [Oct. 2018].

[26] ROBINSON, J, ET AL, J. Robinson, D. Jovcic and G. Joos, "Analysis and Design of an Offshore Wind Farm Using a MV DC Grid," in *IEEE Transactions on Power Delivery*, vol. 25, no. 4, pp. 2164-2173, Oct. 2010. [Oct, 2018].

[27] Pyrhonen Et Al. *Design of rotating electrical machines*, Wiley, 2014.

[28] Dokić B. And Blanuša B., *Power Electronics Converters and Regulators*, Springer, 2007.

[29] C. Busca, A. Stan, T. Stanciu and D. I. Stroe, "Control of Permanent Magnet Synchronous Generator for large wind turbines," *2010 IEEE International Symposium on Industrial Electronics*, Bari, 2010, [Sept. 2018]

[30] W. Chen, A. Huang, S. Lukic, J. Svensson, J. Li and Z. Wang, "A comparison of medium voltage high power DC/DC converters with high step-up conversion ratio for offshore wind energy systems," *2011 IEEE Energy Conversion Congress and Exposition*, Phoenix, AZ, 2011 [Aug. 2018].

[31] Erickson and Maksimović, *Fundamentals of Power Electronics*, Kluwer, 2001.

[32] N. Denniston, A. M. Massoud, S. Ahmed and P. N. Enjeti, "Multiple-Module High-Gain High-Voltage DC–DC Transformers for Offshore Wind Energy Systems," in *IEEE Transactions on Industrial Electronics*, vol. 58, no. 5, pp. 1877-1886, May 2011 [July 2018].

[33] S. Fan, T. Lim, H. Zhang, S. Finney and B. Williams, "Design and control of wind energy conversion system based on resonant DC/DC converter," *IET Conference on Renewable Power Generation (RPG 2011)*, Edinburgh, 2011, [July 2018].

[34] Richard Gagnon And Jacques Brochu (Hydro-Quebec), "Wind Farm - Synchronous Generator and Full Scale Converter (Type 4) Average Model", Internet: https://es.mathworks.com/examples/simpower/mw/sps_product-power_wind_type_4_avg-wind-farm-synchronous-generator-and-full-scale-converter-type-4-average-model?s_tid=srchtitle. [Sept. 2018]

[35] Commission Regulation (EU) No 548/2014 of 21 May 2014 on implementing Directive 2009/125/EC of the European Parliament and of the Council with regard to small, medium and large power transformers, Internet: https://eur-lex.europa.eu/legal-content/eng/TXT/PDF/?uri=CELEX:32014R0548&from=EN ,2009 [Dec. 2018].

[36] X. Yang, D. Patterson and J. Hudgins, "Permanent magnet generator design and control for large wind turbines," *2012 IEEE Power Electronics and Machines in Wind Applications*, Denver, CO, 2012, [Sept. 2018]

[37] Z. Q. Zhu and D. Howe, "Influence of design parameters on cogging torque in permanent magnet machines," *1997 IEEE International Electric Machines and Drives Conference Record*, Milwaukee, WI, USA, 1997, [Oct. 2018].

[38] J. Yang, J. O'Reilly and J. E. Fletcher, "An overview of DC cable modelling for fault analysis of VSC-HVDC transmission systems," *2010 20th Australasian Universities Power Engineering Conference*, Christchurch, 2010, [Nov. 2018]

[39] P. Karlsson and J. Svensson, "DC bus voltage control for a distributed power system," in *IEEE Transactions on Power Electronics*, vol. 18, no. 6, pp. 1405-1412, Nov. 2003 [Oct. 2018].

[40] Prysmian, "Catalog of Solutions for Wind Farms", Internet: https://de.prysmiangroup.com/sites/default/files/atoms/files/PGCEE_Wind_lowres.pdf , Sept. 2018 [Nov. 2018].

[41] ABB, "Catalog of semiconductors", Internet: https://new.abb.com/semiconductors/ [Dec. 2018]

[42] NEXANS, Submarine cable Portfolio, 33 kV. Internet: http://www.nexans.co.uk/eservice/UK-en_GB/pdf-product_540145475/2XS_FL_2YRAA_3x1x400_RM_35_19_33_36_kV.pdf [Jan. 2019]

[43] A. Grauers, "Efficiency of three wind energy generator systems," in *IEEE Transactions on Energy Conversion*, vol. 11, no. 3, pp. 650-657, Sept. 1996, [Jan. 2019].

[44] MATHWORKS libraries, "IGBT model", Internet: https://www.mathworks.com/help/physmod/sps/powersys/ref/igbt.html?s_tid=srchtitle , [Jan. 2019]

[45] MATHWORKS libraries, "Linear transformer model", Internet: https://www.mathworks.com/help/physmod/sps/powersys/ref/lineartransformer.html?s_tid=srchtitle , [Jan. 2019].

[46] M. Starke, L. M. Tolbert and B. Ozpineci, "AC vs. DC distribution: A loss comparison," *2008 IEEE/PES Transmission and Distribution Conference and Exposition*, Chicago, IL, 2008 [Dec. 2018].